Permanent terrestrial laser scanning for near-continuous environmental observations

Systems, methods, challenges and applications

Lindenbergh, Roderik; Anders, Katharina; Campos, Mariana; Czerwonka-Schröder, Daniel; Höfle, Bernhard; Kuschnerus, Mieke; Puttonen, Eetu; Prinz, Rainer; Rutzinger, Martin; Voordendag, Annelies

DOI
10.1016/j.ophoto.2025.100094

Publication date
2025

Document Version
Final published version

Published in
ISPRS Open Journal of Photogrammetry and Remote Sensing

ISPRS Open Journal of Photogrammetry and Remote Sensing 17 (2025) 100094

Contents lists available at ScienceDirect

ISPRS Open Journal of Photogrammetry and Remote Sensing

journal homepage: www.journals.elsevier.com/isprs-open-journal-of-photogrammetry-and-remote-sensing

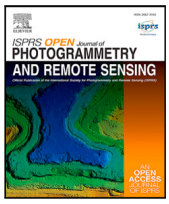

Permanent terrestrial laser scanning for near-continuous environmental observations: Systems, methods, challenges and applications

Roderik Lindenbergh [a,*], Katharina Anders [f], Mariana Campos [e], Daniel Czerwonka-Schröder [h], Bernhard Höfle [g], Mieke Kuschnerus [i], Eetu Puttonen [e], Rainer Prinz [b], Martin Rutzinger [d], Annelies Voordendag [c], Sander Vos [j]

[a] Department of Geoscience & Remote Sensing, Delft University of Technology, Delft, The Netherlands
[b] Department of Atmospheric and Cryospheric Sciences, Universität Innsbruck, Innsbruck, Austria
[c] Institute of Geodesy and Photogrammetry, ETH Zürich, Zürich, Switzerland
[d] Institute of Geography, Universität Innsbruck, Innsbruck, Austria
[e] Department of Remote Sensing and Photogrammetry, Finnish Geospatial Research Institute, National Land Survey of Finland, Espoo, Finland
[f] Department of Aerospace and Geodesy, TUM School of Engineering and Design, Technical University of Munich, Munich, Germany
[g] Institute of Geography, Heidelberg University, Heidelberg, Germany
[h] Department of Geodesy, Bochum University of Applied Sciences, Bochum, Germany
[i] GFZ Helmholtz Centre for Geosciences, Potsdam, Germany
[j] Department of Hydraulic Engineering, Delft University of Technology, Delft, The Netherlands

ARTICLE INFO

Keywords:
Terrestrial laser scanner
Change analysis
Continuous measurements
4D
Topographic monitoring
Time series

ABSTRACT

Many topographic scenes exhibit complex dynamic behavior that is difficult to map, quantify, predict and understand. A terrestrial laser scanner fixed on a permanent position can be used to monitor such scenes in an automated way with centimeter to decimeter quality at ranges of up to several kilometers. Laser scanners are active sensors, and are therefore able to continue operation during night. Their independence from texture conditions ensures that in principle they provide stable range measurements for varying surface conditions. Recent years have seen a strong increase in the employment of such systems for different scientific applications in geosciences, environmental and ecological sciences, including forestry, glaciology, and geomorphology. At the same time, this employment resulted in a new type of 4D topographic data sets (3D point clouds + time) with a significant temporal dimension, as systems are now able to acquire thousands of consecutive epochs in a row. Extracting information from these 4D data sets turns out to be challenging, first, because of insufficient knowledge on error budget and correlations, and, second, because of lack of algorithms, benchmarks, and best-practice workflows. This paper provides an overview of different 4D systems for near-continuous laser scanning, and discusses systematic challenges including instability of the sensor system, meteorological and atmospheric influences, and data alignment, before discussing recently developed methods and scientific software for extracting and parameterizing changes from 4D topographic data sets, in connection to the different applications.

1. Introduction

This work considers permanent laser scanning (PLS) as a method to continuously assess the dynamics of Earth surface topography and vegetation at spatial scan extents in the order of dm to km. Laser scanning is an active sensor technique that uses LiDAR (Light Detection and Ranging) to obtain range distances in different directions from a fixed standpoint, Vosselman and Maas (2010). Laser scanning is more direct and complete in providing 3D surface information than photogrammetry and ground-based SAR (Synthetic Aperture Radar). Photogrammetry requires sufficient texture, lighting, and additional processing from images to 3D information (Förstner and Wrobel, 2016), while ground-based SAR generally relies on the presence of consistent scatterers in a scene (Monserrat et al., 2014).

Conventional 3D monitoring using terrestrial laser scanning (TLS) typically involves the analysis of only a few repeated data acquisitions. Eitel et al. (2016) discussed how at that time laser scanning was transforming into a beyond-3D surveying technique by acquiring more observations than just range distance, like intensity, full waveform or

* Corresponding author.
E-mail address: r.c.lindenbergh@tudelft.nl (R. Lindenbergh).

https://doi.org/10.1016/j.ophoto.2025.100094
Received 23 January 2025; Received in revised form 9 May 2025; Accepted 8 June 2025
Available online 11 July 2025

multispectral signals, or by adding time as a significant dimension. The latter is notably achieved by Permanent Laser Scanning (PLS), also referred to as continuous laser scanning, Bucher and Wertheim (2000), automated terrestrial laser scanning, Kromer et al. (2017), long-term laser scanning, Montillet et al. (2024) and permanent terrestrial laser scanning, Voordendag et al. (2022). In the case of PLS, the scanner is installed in a defined position (fixed or remountable), enabling a continuous acquisition of data, at discrete intervals, over a defined period of time. This review paper focuses on scientific environmental monitoring by PLS systems, excluding indoor and infrastructure applications, as the latter applications pose significantly different requirements to both system setup and consecutive 4D information extraction. In addition, focus is on systems that operate from a fixed stand-point, that is, systems that also scan in a near-continuous way, but from a moving platform, are not considered here.

Terrestrial scanners, implementing both a rotating laser beam and rotating sensor head, acquire range measurements in arbitrary directions. Most often, terrestrial laser scanning is used by combining different scan positions to avoid occlusion and thus fully cover a scene. Permanent laser scanning allows to effectively acquire many (tens to tens of thousands) consecutive scans of the same dynamic scene, which means that PLS enables to observe and quantify ongoing changes rather than just quantifying the net result of composite past changes. Recent years saw the implementation of several PLS systems, which lead to the availability and first experiences with 4D, i.e. 3D plus time, point clouds with a significant temporal dimension.

The availability of these 4D point clouds raised new challenges which starts with the need to handle big data in terms of storing and processing. Methodologically these challenges include multi-temporal point cloud registration and change detection on time series with high temporal resolution. A permanent setup does not guarantee that scans from different epochs are well aligned. Indeed, platform movement, self-heating and atmospheric effects result in alignment differences which make a proper registration procedure necessary. In addition, even after registration, these same effects are still affecting the point cloud quality, but to what extent is specific for different setups. Another challenge is a lack of methodology to extract information on change patterns from time series of consecutive point clouds: existing methodology typically focuses on comparing two epochs, i.e. point clouds from before and after an event, and thereby lacks in exploiting the temporal continuity that time series of scans offer. Both sensor systems and data processing methods that were developed in recent years were constructed with a particular application in mind, which raises the question to what extent methods and setups are transferable to different situations.

This paper is, to the best of our knowledge, the first systematic overview of systems, methods and applications of PLS. In the remainder of this paper, we will first discuss system setup in terms of preparation, installation and data management in Section 2. This section also provides an overview of past and present operational PLS systems, including a table of Open Source PLS data. Section 3 discusses different registration strategies for aligning multi-temporal PLS data and the effect of atmospheric and meteorological conditions on PLS data quality. Section 4 provides an overview of methodology for extraction of change information from 4D PLS data, concluded by a list of Open Source tools implementing some of these methods. Four operational PLS systems, their data products, and data analysis results are showcased in Section 5, followed by a discussion and outlook in Section 6.

2. PLS system setup

This chapter discusses PLS systems, starting by considering design choices and system installation, before providing an overview of operational systems.

2.1. Preparation

Laser safety and setup. Laser safety is internationally organized via the IEN 60825-1:2014 regulations, Anon (2014). Most topographic scanners are Class 1 and eye safe. Only scanners with ranges above 4 km may employ higher class lasers which are not eye safe, RIEGL (2019a). As for normal TLS measurements, a standard risk assessment is recommended, compare e.g. the European framework Directive 89/391/EEC. Important to consider in long-term scanning setups are changing conditions during the campaign. It can be advantageous to identify visitor and animal densities over the planned measurement period to estimate how often potentially dangerous situations can occur. A laser scanner can be set up on a survey pillar or a specially made console, depending on the location. A consideration is the protection of the measurement setup against affecting weather conditions and other influences limiting measurements, as well as theft or vandalism. Most PLS systems use an additional protection cover that prevents fouling of the laser scanner and therefore repeated cleanup tasks. The protection covers consist of glass domes, Polyvinyl Chloride covers, shelters or small scale sea containers.

Presurvey. Compared to mobile scan measurements, long-term campaigns typically require prepared measurement locations. This includes the provision of power, internet connection, frames/towers, protection measures and permits at the scan location. Selecting a final scan location involves balancing these factors with the need for an optimal field of view to effectively study the area of interest. A presurvey at various locations under varying environmental settings can provide information to obtain the most ideal location and setup. Additional information can be obtained by analyzing preexisting data in combination with virtual laser scanning, e.g., Winiwarter et al. (2022). Presurveys can also be used to detect any problems with the field of view due to housing and other structures around the scan location.

Changing conditions can be hard to determine in advance and may require setup changes during the measurement campaign. Stable objects in the scene, both objects of opportunity and designated targets, are useful to align long-term scan sequences, especially because highly dynamic areas can pose a problem for georeferencing. Care should be taken however in using highly reflective targets in the proximity of the scanner, as these have been reported (Pesci and Teza, 2008) to result in anomalous registration results, or even in sensor damage. Unforeseen changes in the field of view because of shadowing effects and vandalism can shorten the usability of these fixed objects.

2.2. Permanent laser scanner system installation

In this paper, PLS is understood as a cycle of four interacting, distinguishable modules. In Fig. 1, data acquisition, data management, data analysis and finally visualization and reporting are four independent topics of a PLS. While methods for data analysis will be described in Section 4, the three other topics will be described in detail in the remainder of this chapter.

Data acquisition. After setup, relevant data can be collected. This can be as simple as using a repetition function in the laser scanner or more advanced, using a scheduler which instructs the laser scanner on specific times to perform a specific type of scan. Suitable sensors can be chosen based on parameters such as range, beam divergence, object resolution, measurement accuracy or ingress protection (IP) classification and level of automation, depending on use of the system in harsh environments. Regarding data quality, it should be noted that the measurement results of a TLS are subject to various random and systematic deviations that together constitute the error model. There are four categories of systematic errors (Soudarissanane et al., 2011). The description in detail is not the subject of this paper. Notably, the data quality is affected by the procedure used for registration, cf. Section 3.1, of the consecutive scans and the systematic influences in the form of geodetic refraction, cf. Section 3.2.

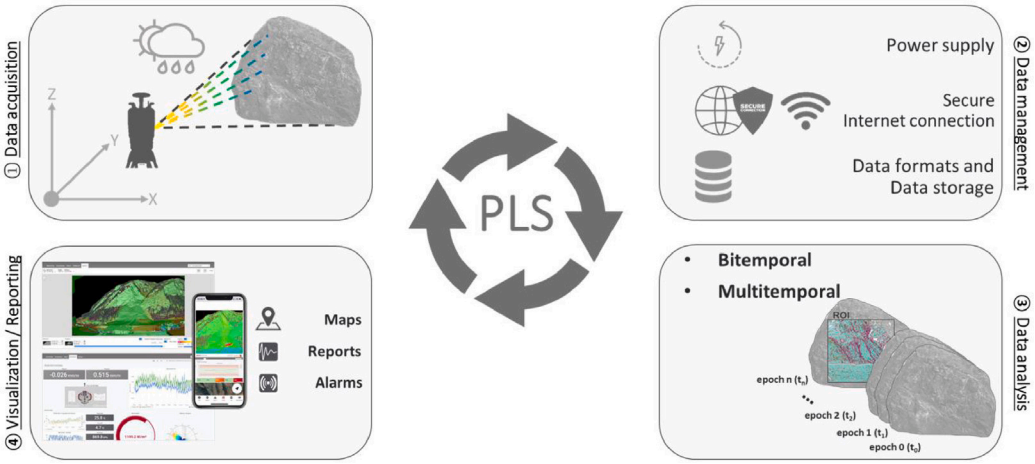

Fig. 1. Workflow PLS design. (1) Data acquisition. (2) Data management. (3) Data analysis. (4) Visualization and Reporting (Czerwonka-Schröder, 2023).

Data management. In terms of PLS integration, open-access data interfaces are offered that enable controlling the scanner using custom-developed software (Czerwonka-Schröder and Gaisecker, 2022). The scanner itself can be remotely controlled via cloud connectivity and enables a continuous stream of data. For example, RIEGL (2024) provides the ROS2 RIEGL VZ Python package to automate laser scanner setup tasks. This includes configuring scan patterns, setting up measurement programs, creating and storing projects on the device, and schedule scan data acquisition, compatible with RIEGL VZ-i series laser scanners, see also (Handl, 2024). Also Livox offers a software development kit to operate their low-cost Livox Avia scanner, compare Ruttner et al. (2023, 2024). Data formats that are both compressed and documented (Pirotti, 2019; Isenburg, 2013) allow the adaptation of own applications to the hardware.

An additional objective of PLS is their autonomous operation. Especially in isolated areas, such as glacier environments (Voordendag et al., 2021), uninterrupted functionality and constant accessibility of the system must be realized. For this reason, a communication gateway should be part of the system to enable both data and energy management. The gateway contains a router that is connected to a central remote evaluation computer via a secure VPN (Virtual Private Network) connection. This ensures that the laser scanner is protected against unauthorized access and is only available to a selected group of people. A so-called watchdog in the communication module performs an automated check of all connected hardware components for their function. In case of irregularities, the watchdog is able to automatically restart the system and inform the system administrator about anomalies. A manual restart of the entire system is also possible. The communication box also offers the possibility of expanding the system with redundant data storage in the form of a NAS (Network Attached Storage) and a backup power supply in the form of a UPS (Uninterruptible Power Supply) as desired.

Data can be stored on the laser scanner, a NAS, the command computer and external backup systems, or on a cloud server. Most times the external backup system/cloud lies outside the physical scan site and requires a data connection to transfer data. Depending on the data connection (fixed internet line, GSM network or beamed data connection), scan data can be repackaged to obtain better control over the transmission lines with limited capability (e.g., in case of a remote observation site) or connection issues, and to decouple the data transmission from the scan cycle. Monitoring in four dimensions (3D + time) poses a significant challenge in terms of data storage and Big Data management. This challenge is particularly pronounced when the phenomena monitored require hourly or daily PLS measurements. For example, Campos et al. (2020) reported a daily data collection of 260 GB.

Reporting and visualization. Finally, the measured values and the information derived should be provided to the stakeholders in an adequate representation. For example, a central data management opens up the possibility of combining the scan data with other sensor data in a web-based monitoring platform, while decision makers typically require a summary of analysis results using only a few key descriptive parameters that can be displayed in colored maps and graphs using web-based tools.

2.3. Operational permanent laser scanners

One of the first operational PLS systems is described in Kellerer-Pirklbauer et al. (2005) were the authors were pioneers in glacier monitoring. Brodie et al. (2012) pioneered the use of a RIEGL LMS-z390i profile system for permanent laser scanning of beach morphodynamics and hydrodynamics in the swash and inner surf zones at the coast in Duck, United States, see also Brodie et al. (2015). The automated use of a Sick profile scanner is discussed for gravel beach monitoring in Almeida et al. (2015), and for estimating wave parameters in the swash zone in Vousdoukas et al. (2014). More recently, Arshad et al. (2021) reports on the setup and use of an automated system build around a Cepta Vista P60 laser scanner to monitor a coastal lagoon entrance at Wollongong, Australia. Abellán et al. (2010), and later (Williams et al., 2018) describe early systems for rockfall monitoring while Kromer et al. (2017) describes a system used to monitor the Séchilienne landslide. Culvenor et al. (2014) describes a system built from scratch around a low cost GLM150 rangefinder for monitoring vegetation structural information to calibrate satellite based Leaf Area Index estimation. Eitel et al. (2013) describe a similar system to quantify 3D temporal dynamics of plant structure.

In recent years, PLS systems were growing in all aspects: in number of systems, in number of acquired epochs and in the variety of their application An overview of recent operational PLS systems reported upon in literature is given in Table 1. From the table, the Hyytiälä site is further discussed in Section 5.1, while the scanner at the Hintereisferner, Austria, is showcased in Section 5.2. Vals is further illustrated in Section 5.3. In the table, CoastScan refers to the same laser scanner that has been active at two different sites in The Netherlands: Kijkduin, for about 6 months, compare also Section 5.4, and Noordwijk, which was operational for 3 years. The same scanner was also operational at Mariakerke, Belgium. Noteworthy is the Field Research Facility (FRF) Duck LiDAR system monitoring the sandy beach at Duck, North Carolina, United States. It was initially deployed in October 2015 and has been collecting hourly scans semi-continuously for the past 9.5 years, with downtime primarily related to scanner issues or servicing.

Table 1
PLS systems, reported upon in literature; countries are indicated by ISO 3166 country code.

Name, country	Scanner	Interval	Epochs	Application	Range	Reference
CoastScan, NL	Riegl VZ-2000	1 h	30 000	Beach	<1 km	Vos et al. (2022)
Mariakerke, BE	Riegl VZ-2000	1 h	8500	Beach	<1 km	Deruyter et al. (2020)
Hintereisferner, AT	Riegl VZ-6000	1 day	850	Glaciology	<4.5 km	Voordendag et al. (2023a)
Hyytiälä, FI	Riegl VZ-2000i	1 h	>25 000	Forestry	<400 m	Campos et al. (2021b)
Séchilienne, FR	Optech ILRIS LR	30'	1832	Landslide	700–1200 m	Kromer et al. (2017)
Whitby, GB	Riegl VZ-1000	1 h	9000	Rockfall	300–550 m	Williams et al. (2018)
Schneeferner, DE	Riegl VZ-2000i	1 h	129	Snow cover	<1 km	Anders et al. (2022)
Vals, AU	Riegl VZ-2000i	2–3 h	1800	Rockfall	<1 km	Schröder et al. (2022)
FRF Duck, NC, US	Riegl VZ-1000	1 h	75 000	Beach	<1 km	O'Dea et al. (2019)
Trier, DE	Riegl VZ-2000i	1 h	>6500	Rockfall	150–400 m	Czerwonka-Schröder et al. (2025)

Table 2
Open Source PLS data. The Pheno4D greenhouse data set in the first row is not obtained by a panoramic laser scanner but by a close-range scanning arm. Pheno4D is included as it is one of the first open source point cloud time series.

Location, country	Years	Interval	Reference	Repository
Duck, US	2015–2025	Hourly	O'Dea et al. (2019)	CHL data server
Greenhouse growing station, DE	2020	Two daily	Schunck et al. (2021)	IPB, Bonn
Kijkduin, NL	2016–2017	Hourly	Vos et al. (2021)	Pangaea
Mariakerke, BE	2017–2018	Hourly	Vos et al. (2024)	Zenodo
Noordwijk, NL	2019–2022	Hourly	Vos et al. (2023)	4TU.ResearchData
Schneeferner, DE	2018	Hourly	Anders et al. (2021a)	heiDATA
Hyytiälä, FI	2020–2021	3.5 days	Wittke et al. (2024)	Fairdata.fi

In Table 1 only a few types of laser scanners are mentioned. Reason is that these scanners were developed for long-range data acquisition with resources for full data acquisition automation and remote connection. Some quality metrics for these scanners are summarized in Table 3. The beam divergence, γ, quantifies the angular increase in beam diameter, and enables to estimate the footprint size, D, as function of range, R, Vosselman and Maas (2010),

$$D \simeq \gamma R. \tag{1}$$

Here it should be noted that Eq. (1), holds in case the laser beam hits the scanned surface perpendicularly. For example, scanning perpendicularly at 1 km with a beam divergence of 0.12 mrad would result in a footprint diameter of 0.12 m. In Table 3, the accuracy refers to the conformity of a range measurement to the real range distance, while the precision indicates to which degree further range measurements obtain the same result. Table 3 on itself provides limited insight in the quality of PLS data, as the effects of measurement geometry, alignment (in)stability and data redundancy are not incorporated. Most PLS systems acquire scans at hourly intervals, thereby providing often data redundancy in terms of the processes that are observed, but also resulting in large data volumes. Ranges are typically in the order of a few hundred meter, only at the glacier called Hintereisferner ranges reach up to 4.5 km, as in this case a full glacier is monitored.

Table 2 provides an overview of open source PLS data. The first data set listed, Duck, consists of hourly beach grids acquired for a period of about nine years on the sandy beach of North Carolina. Pheno4D, provides two long time series of point clouds of maize plants (84 point clouds) and tomato plants (140 point clouds). Corresponding leafs are consistently labeled throughout part of the time series. This data set is obtained by a scanning arm. The consecutive three data sets provide beach topography data at Kijkduin, Mariakerke and Noordwijk, and are obtained by the same scanner, operational at different locations. The Schneeferner data set consists of 125 largely consecutive hourly epochs of snow cover data. The Hyytiälä data set consists of point clouds of 103 different epochs, and covers 458 trees around the scan location.

3. Known PLS data issues

3.1. Registration

Although the scanner position is fixed over time in the case of near-continuous laser scanning, scan results show that alignment procedures

Table 3
Scanner quality, as reported by the manufacturers. Given accuracy and precision values correspond to a 1σ interval and are valid for the indicated range under test conditions as used by the manufacturer.

Scanner	Beam divergence	Accuracy	Precision
VZ-1000	0.3 mrad	8 mm (100 m)	5 mm (100 m)
VZ-2000	0.3 mrad	8 mm (150 m)	5 mm (150 m)
VZ-2000i	0.27 mrad	5 mm (100 m)	3 mm (100 m)
VZ-6000	0.12 mrad	15 mm (150 m)	10 mm (150 m)
Optech ILRIS-LR	0.25 mrad	7 mm (100 m)	4 mm (100 m)

are needed to correctly overlay scans from different epochs. Sometimes there are even alignment issues within one scan. Fig. 2A shows two unregistered scans of the Kijkduin data set, that are obviously tilted w.r.t each other. As a simulated example, consider a PLS positioned 10 m above a flat, horizontal beach. A 1 mm vertical error will result in a 1 cm horizontal error at 100 m horizontal distance of the scanner on the beach. At 1000 m horizontal distance, this horizontal error will have increased to 10 cm. This example shows that small issues in the stability of a measurement setup easily results in rather large errors in the far field. If and how registration is applied, depends on the system setup and on the user requirements. If it suffices to identify changes between consecutive epochs in the order of 25 cm or more, no additional registration effort is needed for any of the systems mentioned in Table 1. At setup it should already be considered if the so-called Scanner Own Coordinate System (SOCS) can be considered stable during scanning. If not, e.g. because the scanner mount is expected to move during scanning due to wind, the movement of the scanner should be, first, tracked, for example on location with an IMU, or relative to an external stable point, and, second, corrected for.

If however the SOCS is considered stable during one scan, it is typically assumed that the point cloud registration problem comes in the form of the estimation of rigid transformation parameters for aligning one point cloud scan to another. Near-optimal transformation parameters between LiDAR point clouds can be obtained by applying different coarse-to-fine registration strategies (Vosselman and Maas, 2010), including feature-based methods (Cheng et al., 2018), global methods such as iterative closest point (ICP), and more recently, learning-based approaches (Monji-Azad et al., 2023) and multitemporal targetless methods, Yang et al. (2025). As still the scanner is operating from a fixed mount, it can be assumed that coarse registration is not required for PLS.

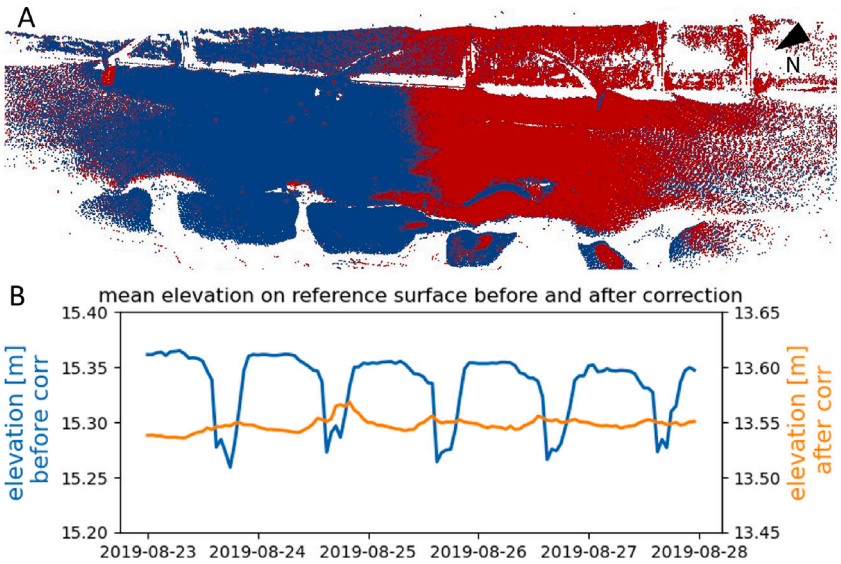

Fig. 2. The need for registration in permanent laser scanning. A: Two unregistered CoastScan point clouds acquired in Kijkduin on January 16 (red points) and January 17 (blue points) 2017. The dominant color (red/blue) shows which point cloud lies on top of the other. Image by authors. B: Time series of the average elevation of a stable reference surface in the CoastScan point clouds, acquired in Noordwijk over one week in August 2019, before and after correction (Kuschnerus et al., 2024a). (For interpretation of the references to color in this figure legend, the reader is referred to the web version of this article.)

What the different registration methods do have in common is that they all require the presence of stable points in or near the scene. To fulfill this requirement, there are different strategies: (i) using natural surface targets, (ii) using prisms at short or long ranges, (iii) using additional sensors, such as total stations. Having natural surface targets is often problematic in highly dynamic environments, like a beach, glacier or forest, without any fixed geometries like a permanent beach pavilion with planar walls, stable rocks around a glacier or some fixed object in a forest. Using dedicated prisms or stable targets might provide an alternative, but even setting up these in a dynamic environment might be challenging.

While either measuring the motion of the scanner through time using inclinometers or by positioning the scanner and its orientation relative to external targets, or by combining both in a common adjustment, a common, time independent coordinate system can be established to which individual scans are aligned.

Different strategies have been applied for aligning PLS data obtained by the systems mentioned in Table 1. For example, Campos et al. (2021b) performed coarse registration of Hyytiälä PLS time series by using a combination of artificial spherical targets and well-defined stable features, such as tree stem positions and corners of man-made structures like research containers and flux towers as Ground Control Points (GCPs). Inclination measurements from the CoastScan laser scanner, available at a frequency of 1 HZ were averaged for each scan except during storms to estimate and correct for mean pitch and roll inclination in Kuschnerus et al. (2024a). After alignment, instantaneous changes of 3 cm could be identified using a statistical approach. Recently, Yang et al. (2025) demonstrated for the PLS site at Vals, that under difficult terrain conditions, and by integrating Total Station measurements, most distances between points at stable areas could be reduced to fall within 1 by a rigid body registration.

3.2. Influence of atmospheric and meteorological conditions

Fig. 2B shows how the elevation (blue line) of a reference surface varies during warm summer days in hourly beach scans. In this particular case, elevation differences (blue line) between day and night are in the order of 10 cm at a range of ~135 m. The elevation difference could be largely reduced (orange line) by a correction for scanner tilt based on inclination angles measured by the scanner.

Meteorological conditions, like rain and wind, have a clear effect on the error budget and data availability of PLS data. Therefore, meteorological conditions need to be taken into account during automated PLS time series processing, e.g. by means of a pre-processing step that automatically removes scans acquired during meteorological less favorable conditions. Storms might influence the stability of the PLS and Kuschnerus et al. (2021b) describes how scans are automatically removed based on evaluation of pitch and roll values of an on-board inclination sensor. Also fog and clouds hinder data acquisition. For example, with the 6 km range Riegl VZ-6000, with wavelength λ = 1064 nm, data acquisition is impossible as soon as clouds are visible between TLS and target surface. For the Riegl VZ-2000i, at λ = 1550 nm, data acquisition is still possible but limited in similar conditions (Campos et al., 2021b). Fig. 3 (A) shows that the maximum range (m) of the Riegl VZ-2000i increases according to the horizontal visibility in the research area. Here, horizontal visibility, in meters, is interpreted as the estimated maximum distance at the weather station that an observer can see an object situated in the same horizontal plane. The maximum range and number of collected points decrease as function of the precipitation amount as presented in Fig. 3(B) and (C), respectively. The increase of the precipitation amount (mm) results in a decrease of number of points (represented by the black line) and, consequently, only the brightest reflectance target responses are registered (represented by the yellow line), increasing the mean reflectance value of a point cloud, expressed in decibels.

Atmospheric effects on scan results are more subtle and often go unnoticed when single scans are obtained at intervals of weeks to months. The scanner measures the time-of-flight between TLS and target surface. The laser beam is delayed by the group index of refraction relative to the speed of light in vacuum (RIEGL, 2019b; Friedli, 2020). This index depends on air temperature, relative humidity, and air pressure between TLS and target surface. Changes in these conditions change the velocity of the laser beam and refracts the beam. To simulate beam velocity and refraction, Friedli (2020), Voordendag et al. (2023a), spatio-temporal high-resolution observations or simulations of the meteorological conditions during scan acquisition are needed. The influence of the atmosphere on the velocity of the laser beam is in the order of millimetres for ranges up to 4.5 km (Voordendag et al., 2023a) and the refraction is approximately 5 cm at a range up to 1 km (Czerwonka-Schröder, 2023) or 25 cm at range up to 2.5 km (Friedli, 2020).

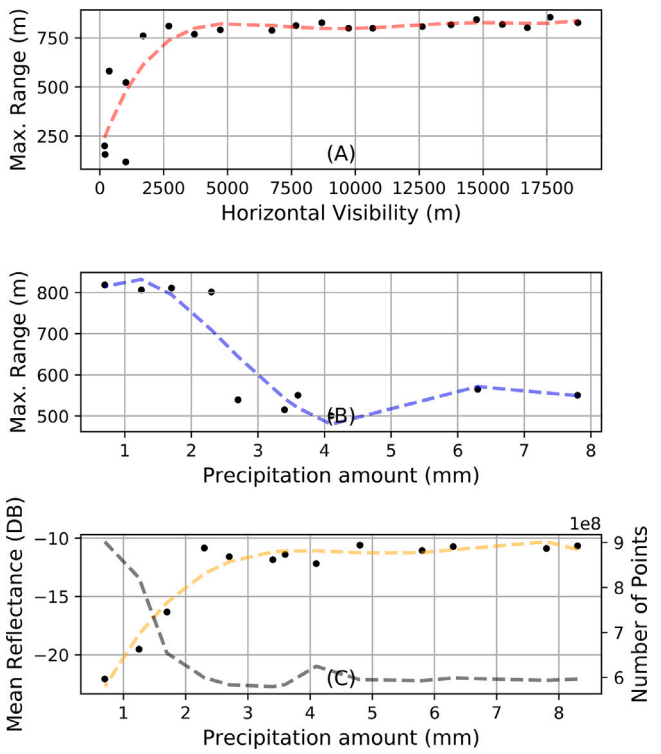

Fig. 3. Effect of weather conditions on Riegl VZ-2000i Hyytiälä, Finland PLS point clouds. (A) Atmospheric horizontal visibility (m) versus maximum detectable point distance. The maximum point detection distance was limited by the scanner mounting configuration., (B) Precipitation amount (mm) versus point cloud maximum range (m), and, (C) Precipitation amount (mm) versus point cloud mean reflectance response (DB) (yellow) and number of points (black). Image by authors. (For interpretation of the references to color in this figure legend, the reader is referred to the web version of this article.)

Refraction increases with strong temperature gradients in the atmosphere, which generally occur closer to the surface. Notably Brocks (1939) showed that the refraction is dependent on the close vicinity of the instrument location, as, depending on the particular setup, there the laser beam is generally close to the surface. He states that in the first tenth of the pathway of the measuring beam the influences are 19 times stronger than in the last tenth. The influence of the atmospheric conditions can be minimized by data acquisition during night for daily acquisition intervals, as the influence of warming of the atmosphere is smaller in the night, and by choosing a setup where the laser beam does not travel close to the surface, especially at the point where the laser beam leaves the TLS.

4. Data analysis and information extraction

The major value of PLS data lies in the temporal dimension of the acquired 3D point clouds. The occurrence of events, like rockfalls, Zoumpekas et al. (2021), can be timed more accurately, while the temporal redundancy enables the detection of small temporal trends. Kuschnerus et al. (2024a) shows how the temporal redundancy of PLS data can be incorporated to identify with statistical significance small vertical jumps and small trends using geodetic adjustment theory. Actually, the 3D time series provide a near-continuous representation of surface processes, and therefore, rather than merely an increase in the number of bitemporal change assessments, these data sets enable a full 4D assessment of ongoing processes. Therefore, new approaches of change analysis in 4D data sets are being developed, that are able to exploit the full time series information to assess dynamic surface processes.

Near-continuous surface or object change is analyzed in either a Lagrangian or in an Eulerian framework, Suchde and Kuhnert (2018). In a Lagrangian framework, the trajectory of objects or object points is assessed, think for example of a rock on a glacier that is moved downstream by glacier flow. Alternatively, dynamic point cloud processing is done using an Eulerian framework, by considering the vertical change at fixed horizontal positions or the range change at fixed spherical positions. This can be, for example, the observation of sediment accumulating and eroding at a fixed location.

In the following sections, we provide an overview of existing methods for 4D point cloud analysis and their application domains. The section concludes by summarizing state-of-the-art Open Source software that implements some of the methods discussed.

4.1. Range acquisitions

A static laser scanner measures a range distance at a certain horizontal and vertical look angle. While scanning, the scanner head rotates around its vertical axis, which corresponds to a change in horizontal scan angle. In addition, the vertical look angle is changed by a rotating mirror. This means that a static laser scanner is acquiring distances in a spherical coordinate system, and these acquired distances could be stored in corresponding raster images. If perfectly stable, PLS would in this way acquire time series in range distance at fixed horizontal and vertical look angles. In practice, cf. Section 3.1, PLS data need registration and laser scanners do not measure range distances at precisely fixed angular intervals. In addition, range distances are often more difficult to interpret than vertical change at horizontal location. As a consequence, most methods analyze PLS data within a Cartesian coordinate system.

4.2. Spatio-temporal interpolation

Spatio-temporal interpolation methods are applied on PLS data for obtaining heights at fixed horizontal positions and for the reduction of noise and uncertainty. In addition, interpolation is used for the filling of spatial or temporal gaps, as caused by variable atmospheric conditions or temporary presence of water on e.g. the intertidal area of a beach. Whereas spatial interpolation is a standard step in topographic point cloud processing, e.g. in creating Digital Elevation Models, compare Ch. 4 in Vosselman and Maas (2010), temporal interpolation, and also temporal aggregation have become relevant through high-frequency acquisition.

To combine filtering in both the spatial and temporal domain, Kromer et al. (2015) use the median of values in a spatio-temporal neighborhood. Therein, spatial neighbors are the n closest points to a 3D point of interest, and the temporal neighbors are the spatially closest points in previous and consecutive epochs. This median averaging is performed for each epoch in a time series, equivalent to a sliding temporal window with a spatial neighborhood search in each epoch within the window. The method has been shown to efficiently reduce noise (i.e., random errors) and can increase the level of detection in change analysis by up to two orders of magnitude. Only averaging in the time domain is used by later applications (Eltner et al., 2017; Anders et al., 2019). This is adequate if spatial interpolation is applied in a separate step. A trade-off must be made between the size of the temporal window and the signal of surface processes being observed. Depending of the relation between temporal resolution of 4D point clouds and the rate of observed surface processes, the signal may be smoothed by temporal interpolation (Kromer et al., 2015).

An approach to fully consider uncertainties in space and time is presented by Winiwarter et al. (2023), who use Kalman filtering for interpolation of a 3D time series. This smoothing of a best estimate time series at locations in the scene enables to reduce the uncertainty of change detection especially for gradual changes and trends in the scene.

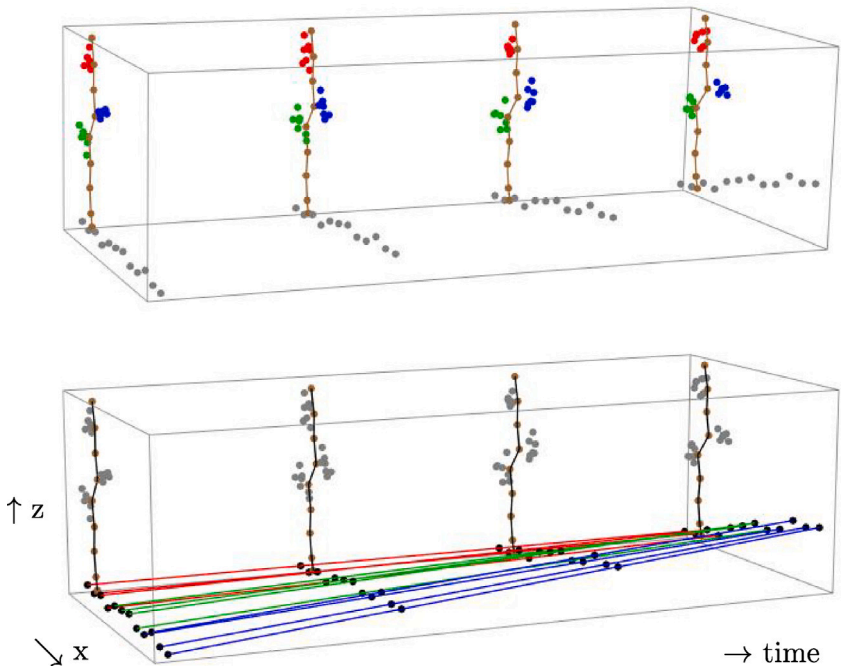

Fig. 4. Spatial vs. temporal clustering. Mock-up of four epochs of 2D point clouds depicting a tree on terrain of varying height. Top: tree parts are clustered spatially, resulting in red, green an blue spatial clusters that can be tracked through time. Bottom: time series of elevation through time at fixed x location are clustered in blue, red and green clusters of time series according to their temporal behavior. Image by authors. (For interpretation of the references to color in this figure legend, the reader is referred to the web version of this article.)

4.3. Systematic trend inventory

Given a set of elevation time series, each series can be systematically analyzed to determine whether the elevation is stable or better described by a linear trend or by another linear model, compare Ch. 7.2 in Vosselman and Maas (2010). Using the statistical framework of adjustment theory, this idea can be formalized, and it can be tested in a statistical way, which linear model under consideration is best, in the sense of least squares, describing the variation in elevation at a grid point. Input is, except for the elevations itself, also the quality of the elevation estimation per epoch, as described by a standard deviation. The sensitivity of the methods depends on both the elevation quality and the data redundancy. Kuschnerus et al. (2024a) applied this approach on PLS data of Noordwijk beach and showed that slopes of 0.032 m/day and elevation jumps of 0.031 m could be identified with statistical power of 80% and with 95% significance in a time series of one day consisting of 24 hourly epochs.

In Kuschnerus et al. (2024b), this method is applied to build a trend inventory of the full three years of hourly PLS data of Noordwijk beach. In this case only linear trends are considered, and partial trends are automatically stopped in case new elevations do no fit the trend under consideration, or in case of data gaps. The resulting inventory consists of 12.8 million partial time series with associated rate of change and elevation. Typically, trends stop in case of high energy events, such as storms or human intervention like bulldozing. This Eulerian method works per grid cell and spatial correlation is not incorporated, but becomes visible in the results as nearby grid cells often exhibit similar behavior.

4.4. Clustering approaches

Clustering is an unsupervised family of methods that groups nearby points based on similar properties, including temporal behavior.

Tracking spatial clusters

Recently, clustering methods have been developed to monitor individual trees (Puttonen et al., 2019; Wang et al., 2022) and vegetated landslides (Weidner et al., 2021) in 3D point cloud time series. These methods are Lagrangian, as they track spatial clusters, representing the same object parts, through time, compare also Fig. 4, top. Vegetated scene monitoring is challenging as plants have complex structure, are non-rigid over time, and their point clouds have various level of incompleteness due to self-shading and occlusions. Puttonen et al. (2019) developed a method based on Euclidean clustering to monitor circadian movements using 14.5 h TLS time series. The initial cluster positions were predefined based on minimum cluster diameter and point number at a selected epoch and all points were given the label of their nearest cluster. The point labels were transferred to subsequently measured point clouds using nearest neighbor search. Following this, the cluster positions were updated before proceeding to the next iteration. The approach was used in detecting and quantifying tree crown dynamics, like branch movement over time. The same method was also applied in a study to determine the driving factors behind circadian branch movements by Junttila et al. (2022).

Wang et al. (2022) developed an algorithm, PlantMove, for non-rigid registration of multi-temporal tree point clouds to monitor structural crown dynamics. PlantMove creates motion fields between consecutive point clouds using the Coherent Point Drift algorithm by Myronenko and Song (2010). The method was successfully tested on three case studies, including two real-world point cloud time series. Chebrolu et al. (2020) developed a non-rigid registration method to phenotype plant organ growth in tomato and maize plants for a ten-day period based on spatio-temporal point clouds. Their method searches for correspondences between object skeleton nodes at different epochs using a Hidden Markov Model formulation.

An object clustering method to monitor changes and deformation in a vegetated landslide based on tree trunk matching from sequential LiDAR point clouds was developed by Weidner et al. (2021). The algorithm, TreeTracker, includes point cloud semantic segmentation (trunk vs. non-trunk), trunk point cloud clustering and centroid calculation,

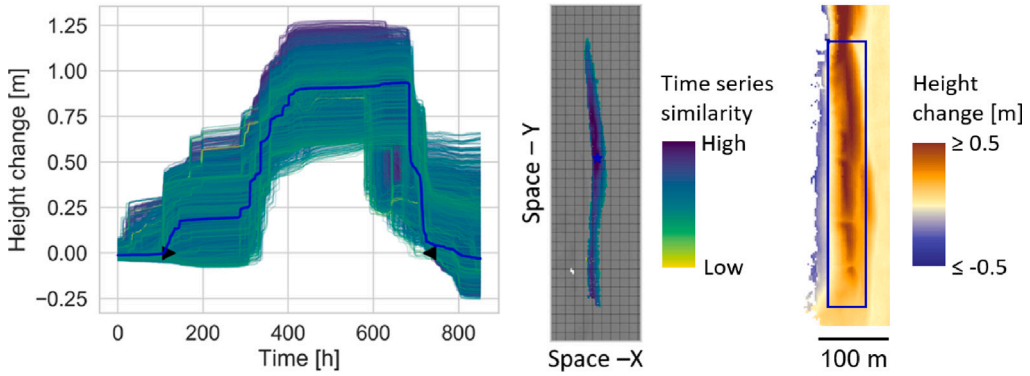

Fig. 5. Example 4D object-by-change represented by a spatially contiguous group of time series (left) which exhibit similar surface behavior throughout the time span of the identified surface activity. The blue line in the left figure indicates the seed time series. The middle figure displays the similarity between time series parts between each location in the object and the seed (location marked by blue star). The right figure shows the height change in the scene compared to the height in a reference epoch, with the object extent in the blue rectangle. Image by authors. (For interpretation of the references to color in this figure legend, the reader is referred to the web version of this article.)

matching of corresponding trees in multi-temporal datasets and 3D displacement estimation of individual trees. Landslide changes and deformation are therefore estimated based on the positions of clustered trunk point cloud centroids over time.

Time series clustering

Instead of following spatial clusters through time, one can also, in an Eulerian approach, group positions in a scene based on time series similarity, compare also Fig. 4, bottom. Similar dynamic processes in a beach dune system were grouped using k-means clustering applied on multi-year coastal airborne LiDAR data (Lindenbergh et al., 2019). Kuschnerus et al. (2021a) used well-known clustering methods (k-means, DBSCAN, agglomerative clustering) on elevation time series from the CoastScan data set in Kijkduin. With this method different locations could be grouped according to their similarity in change pattern. A division in intertidal and aeolian area was visible and regions with dominant anthropogenic changes like bulldozer work could be isolated. Czerwonka-Schröder et al. (2023a) adapted the k-means clustering to a spatial set of PLS time series of the Vals valley and could also automatically extract segments with homogeneous temporal properties. In Czerwonka-Schröder et al. (2023b) a feature-based clustering approach based on a Gaussian mixed model is presented as an alternative to k-means clustering.

4.5. Extraction of 4D objects-by-change

A well-known approach to segment a point cloud is by means of region growing (Vo et al., 2015). Starting from a seed point, spatial neighbors are added to a segment, as long as some homogeneity criterion, like planarity, is met. 3D segmentation by region growing has been generalized to the so-called 4D objects-by-change method for 4D point cloud data in Anders et al. (2020). The concept of a 4D object-by-change is to delineate surface activity in its duration and spatial extent based on similar surface behavior throughout the time span of the activity. Here, surface activity is a general term to describe a temporary process of surface change, which may be any kind of local erosion, deposition or combination thereof. To extract a 4D object-by-change, surface activities are first identified in the time series of surface elevation at a location in the scene. Using one detected time span as seed, the spatial neighborhood is then checked for similar surface behavior in the second step. The used metric for time series similarity is the Dynamic Time Warping (DTW) distance (Berndt and Clifford, 1994). The resulting spatially grouped time series subsets represent the spatio-temporal extent of the 4D object, compare Fig. 5. As a 4D object-by-change to some extent enables to follow a spatial pattern of change through time, this method can be seen as a mixed Eulerian-Lagrangian approach.

The extraction of 4D objects-by-change is fully automated using spatio-temporal segmentation (Anders et al., 2021b). By searching for surface activities in the full time series at all locations in the scene, different change processes can be identified, i.e. activities with variable timing, duration, and magnitude. Different 4D objects-by-change may overlap both in space and time. This is possible because the method may segment a location that is already part of one object into an additional object. This is favorable when analyzing scenes of complex surface dynamics, where material is transported by different drivers so that surface processes overlap and interact. An application example is given in Section 5.4 on the extraction of surface dynamics on a sandy beach.

To characterize extracted surface activities as represented by 4D objects-by-change, Hulskemper et al. (2022) use self-organizing maps (SOMs; Kohonen, 1990) to group change objects based on their spatio-temporal properties, such as their spatial extent, duration and magnitude. This unsupervised clustering approach groups and sorts similar surface activities without requiring predefining properties. Such analysis can provide insight into spatial and temporal patterns of surface dynamics, and allows linking identified surface activities to external drivers.

4.6. Open source tools

Open research software is key to transfer scientific achievements into action as modules in full workflows in academia and beyond. Source codes for 4D point cloud analysis are increasingly shared along with publications and several of those open-source projects underlie a software license which allows for unrestricted use (e.g. GNU LGPL 3.0 or later). As a consequence, workflows can use, compare and combine multiple 4D analysis methods.

LiPheKit

Wittke et al. (2024) provided along with the `LiPheStream v1.0` dataset — an 18-month-long point cloud time series comprising LiDAR data from 458 individual trees — a set of practical scientific tools named `LiPheKit` to support the processing of LiDAR time series. This toolkit includes features such as point cloud reading and writing (in LAZ format), normalization, registration and georeferencing, data resampling, coarse-to-fine point cloud segmentation, and tree parameter estimation (e.g., tree height).

PlantMove

Point clouds of the same target collected at different epochs can be compared using the `PlantMove` open-source tool (Wang et al., 2022). `PlantMove`, which includes MATLAB source code and a compiled executable with a graphical user interface, was initially designed to

Fig. 6. Examples of permanent laser scanning systems: (A) PLS at the Hyytiälä Research Forest Station in Finland, used for monitoring tree dynamics; (B) PLS at Hintereisferner, Austria, employed for glaciological studies; (C) PLS at the Trierer Augenscheiner, Germany, for rockfall monitoring; and (D) PLS at Kijkduin, Netherlands, for coastal monitoring. Images by authors.

accurately estimate point-wise 3D motion fields for plant movements based on point cloud time series recorded over time intervals ranging from hours to years.

Py4dgeo - library for change analysis in 4D point clouds

The main objective of the scientific software `py4dgeo` (Py4dgeo Development Core Team, 2022) is to provide an open-source platform and easy to use but performing and flexible tool to run state-of-the-art change analysis methods for 3D time series of point clouds. `py4dgeo` is a C++ library with Python bindings and bundles methods, such as the standard M3C2 algorithm (Lague et al., 2013), M3C2 with error propagation, M3C2-EP, Winiwarter et al. (2021), 4D objects-by-change (Anders et al., 2021b), and the correspondence-driven plane-based M3C2 (Zahs et al., 2022). Also registration methods, including standard ICP and supervoxel-based targetless registration, Yang and Schwieger (2022), have been made available. Thereby, py4dgeo offers a well-defined API to be included in automatic workflows (e.g. online on scanners) and to be used to develop ensemble workflows combining multiple change analysis methods. The library is actively under development in several (inter)national projects.

5. PLS case studies

This chapter will discuss four representative and intensively investigated environmental applications of permanent laser scanning: tree monitoring, glaciology, rockfall and coastal monitoring. The different systems are displayed in Fig. 6.

5.1. LiPhe tree monitoring - Hyytiälä

Understanding forest dynamics is essential to improve sustainable forest management, forest productivity, reforestation, and to protect forests from extreme conditions. Yet, forest dynamics is a complex subject with inter-individual variability according to species, genetic differences, tree age and size, and seasonal environmental interactions (Marchand et al., 2020). Therefore, long-term monitoring at monthly or daily intervals is required to assess forest dynamics. Among the remote sensing sensors, laser scanning systems have become a standard technology for forest monitoring. The high penetrability of the laser beam in tree crowns, the scanner ability to acquire multiple returns per transmitted pulse, and its possibility to measure without external lighting enable investigation of structural development and dynamics of a tree. However, until present, there has been a lack of permanent laser scanning systems that continuously collect point cloud time series at, say, daily intervals. With this motivation, the Finnish Geospatial Research Institute (FGI) developed a LiDAR phenology station (LiPhe) to monitor daily and seasonal changes in a boreal forest (Campos et al., 2021b).

The LiPhe station consists of a time-of-flight Riegl VZ-2000i scanner installed in a fixed support frame near the top of a 35-metre tower ~15 m above the forest canopy. The tower is situated at a Hyytiälä forest research station in central Finland (61° 51′N, 24° 17′E). PLS data acquisition is fully automated and a new scan is measured every hour at 0.006° angular resolution. The LiPhe station has been operational

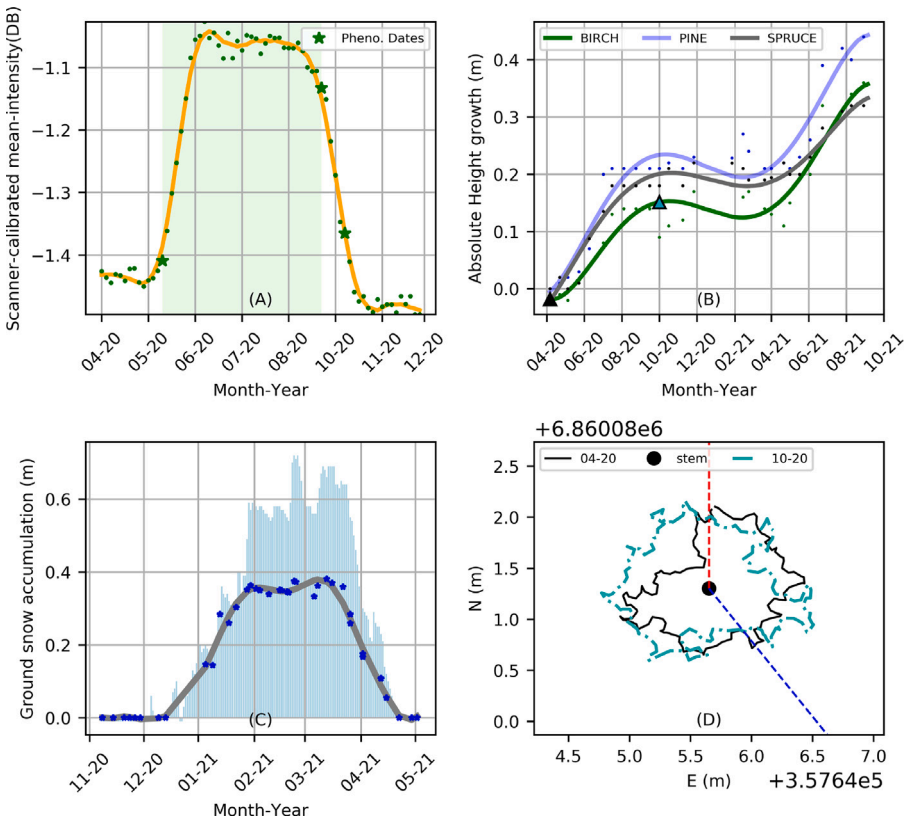

Fig. 7. FGI LiPhe station sample cases: (A) Phenological change detection of a silver birch tree based on scanner-calibrated intensity variation over time, (B) tree height increase of silver birch, Scot pine and Norway spruce trees for the 2020 and 2021 growth seasons, (C) PLS detected ground snow accumulation under silver Birch tree compared to FMI reference data, and (D) silver birch tree area growth over the 2020 growth season. Images by authors. (For interpretation of the references to color in this figure legend, the reader is referred to the web version of this article.)

since April 2020, except for nine months between September 2021 and June 2022 due to hardware failure.

The scan area covers 19 hectares of mixed, conifer dominated, boreal forest. The PLS monitors over 4000 individual trees within 400 m distance from the scanner. A data processing framework converts individual scans into a georeferenced point cloud, labeled with a local tree map to enable analysis of daily and seasonal dynamics at tree level. The LiPhe station time series data set enables the study of dynamics like seasonal growth of tree height and crown area (Campos et al., 2023; Yrttimaa et al., 2024; Campos et al., 2024), variation in biomass (Spadavecchia et al., 2023), snow accumulation and shedding, and phenological date estimation over several seasons (Campos et al., 2021a). Additionally, LiPhe data has been used, Shcherbacheva et al. (2024), to study phenological trends as revealed by annual calibrated LiDAR intensity patterns for tree species classification of Scots pine (*Pinus sylvestris*), Norway spruce (*Picea abies*) and Silver birch (*Betula pendula*) trees.

Fig. 7 shows different tree dynamics for the 2020–2021 growth season. Fig. 7(A) shows the 2020 LiDAR-calibrated intensity pattern of a silver birch tree (in orange), as induced by the tree phenological change over the season. The green dots show the tree averaged values of LiDAR-calibrated intensity at 133 time points. Phenological dates, such as the beginning of the greening and falling, and the end of the season (green stars) correspond to characteristic changes in this intensity response. Fig. 7(B) shows the annual height growth in Scots Pine, Norway Spruce, and silver birch trees based on changes in their 99.95 height percentile in 133 time points. The two triangles in the birch growth curve are times for which the crown area is plotted in Fig. 7(D). The silver birch crown area growth was detected using 2D alpha shapes of point clouds acquired in April (black) and October (cyan) 2020. The tree stem position is represented by a black dot while the red and blue dotted lines show the direction towards North and the scanner position, resp. Finally, Fig. 7(C) presents the ground snow accumulation under a silver birch tree by a gray curve, which is consistent with snow depth values estimated by the Finnish Meteorological Institute (light blue bars).

The LiPhe PLS point clouds and derived tree dynamics analysis are validated with multiple independent measurements. Reference data include a field survey-based tree map, hundred-point dendrometers that monitor seasonal variance in stem width and localized temperature, and two LIDAR helicopter campaigns in August 2021 and 2022. The LiPhe station has been installed in the immediate vicinity of the Station for Measuring Ecosystem-Atmosphere Relations - SMEAR II (Hari and Kulmala, 2005) that monitors the ground-forest-atmosphere continuum. This enables combined studies on how individual tree dynamics varies with changing environmental conditions. Therefore, this PLS time series provides a unique spatio-temporal dataset to better understand long-term dynamics in boreal forests and the impact of changing environmental conditions. An extensive description of the project is also provided in Wittke et al. (2024).

5.2. Glaciology - Hintereisferner

At Hintereisferner (HEF), a valley glacier in the Ötztal Alps, Austria, a Riegl VZ-6000 was installed in September 2016 at an altitude of 3250 m a.s.l. (Voordendag et al., 2021). The system is automated since June 2020 and acquires daily point clouds for deriving Digital Elevation Models (DEMs) of the glacier and its surrounding. The installed scanner is able to scan ranges up to 6 km, but ranges up to 4.5 km are reached at this location. The setup was installed to study glacier surface mass balance processes at high temporal and spatial resolution such as snow (re)distribution over the glacier surface (Voordendag et al., 2024), but

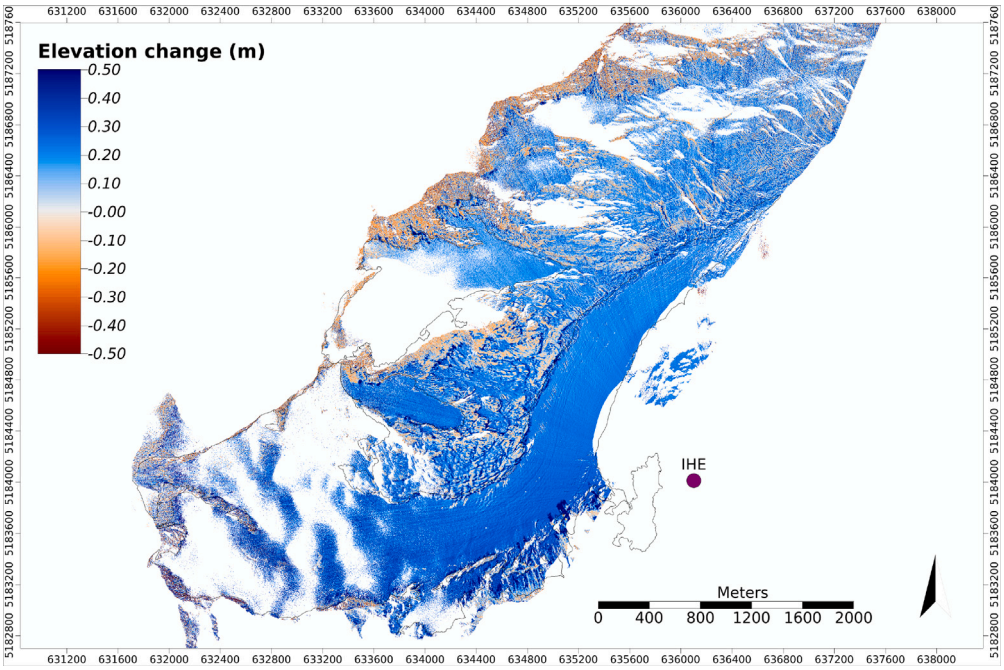

Fig. 8. DEM of difference between 13 and 16 November 2021 as obtained from the Hintereisferner PLS system. The black lines are the glacier outlines of 2018 (Federal Government Tyrol). The research station with the PLS *Im Hinteren Eis (IHE)* is the purple dot. Image by authors.

is also used to distinguish annual and seasonal glacier mass balances, determine the Glacier Loss Day (Voordendag et al., 2023b), and serve as surface boundary condition for glaciological and atmospheric models requiring high resolution in space and time. Fig. 8 shows a DEM of Difference (DoD) between November 13 and 16, 2021. Between those two dates snowfall was registered at a nearby automatic weather station. Thus, the DoD shows the distribution of the snowfall as well as snow redistribution thereafter. Note that not the entire glacier surface area is covered by the station, as the upper part of HEF lies higher than the scanner's position, leading to some scan occlusions (white areas) in Fig. 8. DoDs similar to Fig. 8 are valuable calibration and validation information for atmospheric models that model solid precipitation and snow drift (Goger et al., 2022; Voordendag et al., 2024).

The installation of a PLS system at high altitude in harsh conditions faces additional challenges. This TLS is installed in a small, heated container with mechanical windows that are opened before data acquisition starts (Voordendag et al., 2021). It was found that mechanical problems occurred below −15 °C, so data acquisition is not possible yet below these temperatures. The power supply comes from the nearby ski resort *Alpin Arena Schnals/Senales* (South Tyrol, Italy). Due to missing long-term evolution standards for wireless broadband connection at the time of installation (2016), the remote access is provided through the wireless communication network of the civil protection agency of the Autonomous Province of Bolzano/Bozen, Italy, via Virtual Private Network (VPN) tunneling to the University of Innsbruck. The bandwidth is quite small, but rather stable and splitting the TLS data files into small chunks assures reliable data transfer.

5.3. Rockfall - Vals

A rockfall occurred in the Vals valley in Tyrol, Austria on 24 December 2017, leaving a large debris cone at the lower part of the Alpine slope. According to Berger et al. (2021), about 117,000 m^3 of rock volume was displaced. Using two laser scans conducted in 2008 and on 27 December 2017, immediately after the event, Anegg and Fritzmann (2019) estimate the volume of the deposit at 130,000 m^3, the deposit area at 50,000 m^2, the falling height at 380 m, and the maximum depositional thickness at 9 m. The event loosened the material, corresponding to a volume increase of about 11.5% (Hartl, 2019). Although there were no human casualties or significant damage to buildings, the Valser national road located immediately below the rockfall was covered with 8 m of debris (Hartl, 2019). The local authorities set up a geodetic monitoring system, consisting of a total station with 21 corresponding prisms and geotechnical sensors distributed over the source area of the rockfall on the upper mountain slope in 2018. As no significant rock movement was detected in the acquired data, the infrastructure of the existing monitoring system was made available for research. Point clouds of the rockfall and debris area below were recorded periodically with a Riegl VZ-2000i laser scanner during three measurement campaigns, as specified in Table 4.

Table 4
Scan campaigns at Vals, Austria.

Campaign	Date	Year	Scan interval
M1	13/8 - 8/9	2020	2 h
M2	10/5 - 17/6	2021	3 h
M3	28/7 - 17/12	2021	3 h

During the campaigns, the laser scanner was permanently installed on a survey pillar in a shelter on the opposite slope at ~800 m from the rockfall area, cf. Fig. 9. A high-resolution scan was acquired at 15 mdeg resolution in azimuth and elevation at a pulse repetition rate of 50 kHz. 1780 individual scans were acquired (Schröder et al., 2022). The acquisition was designed for various research and development activities regarding the deployment of long-range terrestrial laser scanners within a remotely controlled, web-based monitoring system from an engineering geodetic perspective (e.g. Gaisecker and Schröder, 2022; Kermarrec et al., 2022; Czerwonka-Schröder et al., 2023b; Winiwarter et al., 2023). In addition to the laser scanner, a Leica TM30 total station (TS) and inclination sensors on the survey pillar aligned to the scanner-own coordinate system, were employed. Various meteorological sensors were installed in the shelter and around the monitored slope area. The additional measurements are used to verify diurnal and seasonal systematic effects on the results of surface change quantification. Notably, the total station was measuring prisms installed in nearby stable rock. As the prisms could be detected as well in the laser scans, PLS-TS correspondences could be used to verify different methodical

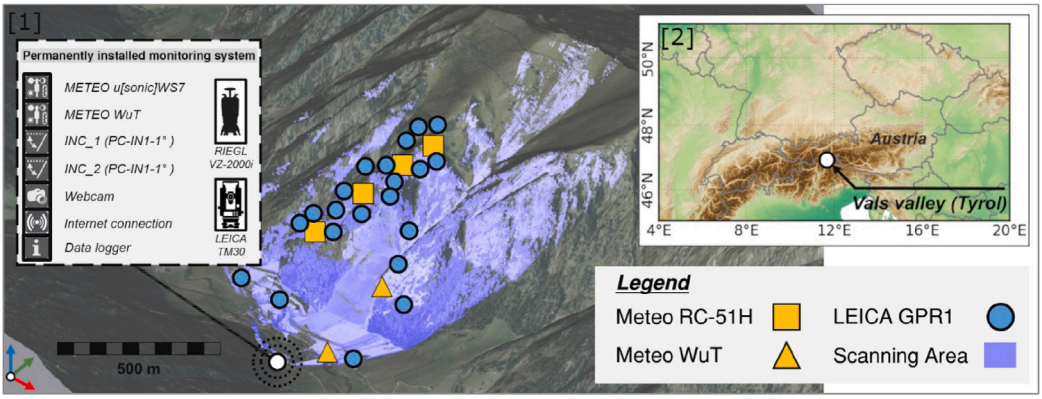

Fig. 9. 3D overview of the test site in the Vals Valley including applied sensor technology and a view of the geographical situation of the Vals Valley (Schröder et al., 2022).

approaches. A comprehensive description of the measurements and the various studies can be found in Czerwonka-Schröder (2023).

5.4. Coastal monitoring - Kijkduin

In Kijkduin, the Netherlands, a Riegl VZ-2000 was installed in December 2016 for a duration of six month to regularly collect point clouds of the dunes and sandy beach. The laser scanner was mounted on a steel frame on the roof of a hotel overlooking the coast. Data was collected every hour at 30 mdeg angular spacing and once per day at noon at a higher angular spacing of 15 mdeg. The resulting 4D spatio-temporal data set is publicly available (Vos et al., 2021) and is described in detail by Vos et al. (2022).

The laser scanner was installed on top of a hotel on a pole stabilized by four cross-braced legs. The scanner was protected against fouling and temperature extremes by a double layer Polyvinyl Chloride housing that needed cleaning only every other three months. Scans were initiated by a command computer which used an adjustable daily schedule. Weather information consisting of atmospheric temperature, pressure and relative moisture, was obtained from online sources for use by the instrument to account for varying atmospheric influences on the range measurements.

A plot showing elevation changes on the beach and dune area between two epochs, before and after a 10-day stormy period at the end of February 2017 is shown in Fig. 10, top. A large eroded area in the intertidal area is visible in red, as well as some smaller sand depositions on the beach, marked with blue arrows. Anthropogenic changes, probably bulldozer works to clear access paths, are the most likely cause of the larger sand deposition marked with a red arrow in Fig. 10.

From the same data set, two time series are shown in Fig. 10, bottom, left. The location of the two time series is indicated on a LiDAR reflectance plot, in Fig. 10, bottom, right. The yellow time series is from a location on the dry beach and shows a sudden height jump of about 20 cm around February 8. Such sudden increases at the dry beach are often human induced. A possible interpretation is that the height jump is caused by a bulldozer creating a sand embankment as preparation for the summer season. The blue time series is from a location in the intertidal area and shows two peaks of over 50 cm high. These dynamics are probably caused by sand banks moving along shore.

The examples above show that it is often difficult to interpret the underlying processes from one single time series. Spatio-temporal context, i.e. what is happening close-by both in space and time, might help interpretation. Such context is for example provided by 4D objects-by-change, compare Fig. 5. The example in the figure in fact contains the location and extent of the first temporal part of the blue time series in Fig. 10, bottom, left.

Fig. 10, bottom right, shows the recorded reflectance from one single scan. Higher on the beach, sand is dryer and reflectance is higher. A full study of reflectance variations and its relation to beach moisture has been published in Jin et al. (2021a,b).

This Kijkduin data set has been analyzed to find geomorphological processes using time series clustering by Kuschnerus et al. (2021a). Anders et al. extracted geomorphological processes using 4D objects-by-change (Anders et al., 2020, 2021b), which have been classified and grouped by Hulskemper et al. (2022). Van IJzendoorn et al. (2024) used Fourier analysis to identify and consecutively track periodic bedforms in the follow-up data set of Noordwijk beach.

6. Discussion and future directions

The above chapters provided an overview of the current state of PLS. Here we discuss expected future directions of PLS.

Multisensor system setup and multimodal processing

One of the strong points of PLS is its ability of near-continuous data acquisition. At the same time this has the consequence that it is sometimes difficult to interpret what effects affect the PLS data. Therefore, while setting up a PLS system, it should be considered what sensors should be installed in addition to the PLS system itself. In situ weather station data can be both used as input to automatically filter PLS data during storms and as morphological forcing data. An additional camera can be used to automatically validate dynamic processes, like bulldozer induced changes on a sandy beach in Barbero-García et al. (2023). For vegetation monitoring, integration with spectral data is expected to be highly beneficial.

The near-continuous data acquisition of PLS makes its data also suitable to calibrate and interpret satellite and airborne data from similar of complementary sensors. Initial results, cf. Di Biase et al. (2022), show how surface roughness as derived from PLS data is correlated to the backscatter of Sentinel 1 radar data, while in Kuschnerus et al. (2024b) PLS data and derived changes at hourly and daily intervals is compared to a 'traditional' yearly change analysis as derived from airborne LiDAR data.

Online big data processing and adaptive monitoring

In Section 4, we provided an overview of recent methodology to extract information from 4D PLS data. So far, method development has been driven by the availability of data at particular sites and by the dominant research questions at these sites, that is, methodology was typically domain driven, and one particular method was used to answer one particular research question. The current availability of these different methods, in description, but also as open source tools does, however, allow to combine them in composed workflows, for example a 4D PLS data set could be clustered first using time series

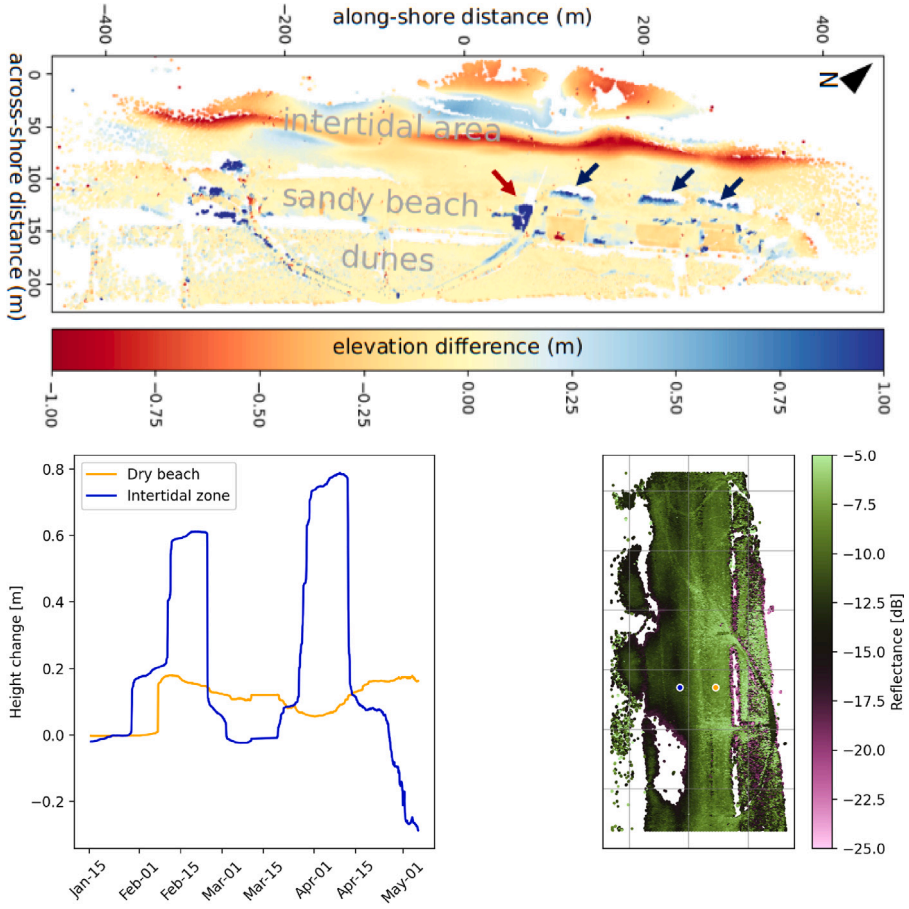

Fig. 10. Top: Elevation change at Kijkduin beach between low tide on 19-02-2017 and 03-03-2017, before and after a stormy period of 10 days. The dunes, sandy beach and intertidal area are indicated. The dark blue arrows indicate sand deposition as a result of the storm. The red arrow points to an area possibly changed by bulldozer works. Bottom: (a) Time series of height change at two locations on the beach derived from six months of PLS point clouds acquired in 2017. (b) Locations of the time series in (a) on the beach, visualized on a point cloud colored by LiDAR reflectance. Grid width of the map is 100 m. Image by authors. (For interpretation of the references to color in this figure legend, the reader is referred to the web version of this article.)

clustering, followed by a 4D-Objects-By-Change analysis of a more dynamic cluster.

What is still largely lacking, as far as we know, are tailor made methods for visualization of 4D PLS data. Methodology is under development, Zhang et al. (2020), Fouché et al. (2023), for related data. In addition, presented methods for information extraction from PLS data are focusing on post-processing. For critical monitoring projects, real-time analysis is required to provide timely warnings. In addition, real-time analysis of ongoing dynamics, may be used to adapt monitoring settings such as acquisition frequency or area of interest. Some existing methods, such as the Kalman filtering approach in Winiwarter et al. (2023) and the systematic trend analysis in Kuschnerus et al. (2024b) should be relatively easy to use in real-time approaches.

Multi-epoch point cloud data

This paper is focused on PLS data, but the discussed methodology is probably in general able to extract information from multi-epoch point cloud data, although there have only been limited attempts to do so. Malsam et al. (2021) describes a semi-automatic workflow to detect rockfall events from a TLS dataset consisting of ∼50 epochs. Both large-scale airborne LiDAR campaigns and more focused UAV LiDAR and photogrammetry campaigns are quite common and should in many cases result in multi-epoch point clouds or Digital Terrain Models (DTMs). Once the number of epochs is 3 or higher, using some of the discussed methods may be beneficial above a more traditional consecutive cloud to cloud or DEMs of differences, James et al. (2012), approach.

Deep learning methodology

Deep learning has started to be applied to point cloud time series, in particular in the field of autonomous driving (Gojcic et al., 2021; Kreutz et al., 2023), but less in environmental research and not yet to topographic PLS. A possible explanation is that multi-temporal environmental geometric objects are yet poorly understood. As a consequence, focus is more on defining and understanding them in the first place, rather than finding back already known multi-temporal objects in a 4D point cloud. The latter could be the equivalent of instance segmentation in 2D or 3D for which many Deep Learning methods have been developed in recent years. Deep Learning could also play a role in tracking spatial objects through time. Notably, instance segmentation is useful in partitioning point clouds into single components, before tracking, e.g. in phenotyping studies (Hao et al., 2024).

7. Conclusions

In this paper we have provided, to the best of our knowledge, a first comprehensive overview of permanent laser scanning (PLS). Such systems are able to autonomously acquire point cloud data in a near-continuous mode, resulting in time series of hundreds to tens of thousands of consecutive point clouds. System setup has been discussed, consisting of a planning phase including presurvey, an installation phase, with special attention to system stability, power management and automation of data acquisition, and an operational phase, where data is delivered to stakeholders. An overview is given of known

PLS setups, including their application and links to open-source data publications.

Using the resulting 4D spatio-temporal point clouds typically requires automated removing of point clouds acquired during poor meteorological conditions (wind, rain) and a fine registration step, often followed by some sort of spatio-temporal interpolation. The high temporal availability of consecutive scans revealed issues with laser scanning caused by different atmospheric and meteorological effects, that often stay unnoticed in traditional scan campaigns. In recent years, several methods have been developed that extract information from 4D data, not in a consecutive bi-temporal way, but by considering the full multi-temporal character of the data. Methods can be distinguished in being Eulerian, where changes at fixed location are considered, or being Lagrangian, where the trajectory of points or objects through time are followed. Both methods and systems are illustrated in four different cases, considering tree monitoring, glaciology, rockfall monitoring and coastal scanning.

Several methods are being made available to the science community as open source software tools, but common use of these methods is still largely lacking. This paper has been focusing on using permanent laser scanning for environmental monitoring. It is expected that PLS systems will also be applied for monitoring structural projects, such as open pit mining or construction sites, while parallels with related monitoring techniques, such as automated photogrammetry or InSAR, could further enrich method and application development.

CRediT authorship contribution statement

Roderik Lindenbergh: Writing – original draft, Methodology, Conceptualization. **Katharina Anders:** Writing – original draft, Visualization, Investigation. **Mariana Campos:** Writing – original draft, Visualization, Investigation. **Daniel Czerwonka-Schröder:** Writing – original draft, Methodology, Investigation. **Bernhard Höfle:** Writing – review & editing, Validation, Supervision. **Mieke Kuschnerus:** Writing – original draft, Methodology, Investigation. **Eetu Puttonen:** Writing – review & editing, Validation, Supervision. **Rainer Prinz:** Writing – review & editing, Validation, Supervision. **Martin Rutzinger:** Writing – review & editing, Validation, Supervision. **Annelies Voordendag:** Writing – original draft, Methodology, Investigation. **Sander Vos:** Writing – original draft, Investigation, Data curation.

Declaration of competing interest

The authors declare that they have no known competing financial interests or personal relationships that could have appeared to influence the work reported in this paper.

Acknowledgments

B. Höfle and D. Czerwonka-Schröder were supported by the Bundesministerium für Bildung und Forschung (BMBF), Federal Ministry of Education and Research, grant 02WDG1696, in the framework of project AIMon5.0. M. Campos and E. Puttonen were supported by the following projects from the Research Council of Finland: (i) Upscaling of carbon intake and water balance models of individual trees to wider areas with short interval laser scanning time series, grant 316096; (ii) Forest-Human–Machine Interplay - Building Resilience, Redefining Value Networks and Enabling Meaningful Experiences, grant 337656, and, (iii), Scan4est: Measuring Spatiotemporal Changes in Forest Ecosystem, under grant 337811. M. Kuschnerus and S. Vos were supported by the Netherlands Organization for Scientific Research, grant 16352, as part of the Open Technology Programme and by Rijkswaterstaat (Dutch Ministry of Infrastructure and Water Management). K. Anders is indebted to the Baden-Württemberg Stiftung for the financial support of the research project CharAct4D by the Eliteprogramme for Postdocs and is supported by the Deutsche Forschungsgemeinschaft (DFG, German Research Foundation) – grant 535733258 (Extract4D project). A. Voordendag was funded over the project "Measuring and modeling snow-cover dynamics at high resolution for improving distributed mass balance research on mountain glaciers", a joint project fully funded by the Austrian Science Foundation (FWF; project number I 3841-N32).

References

Abellán, A., Calvet, J., Vilaplana, J.M., Blanchard, J., 2010. Detection and spatial prediction of rockfalls by means of terrestrial laser scanner monitoring. Geomorphology 119 (3–4), 162–171.

Almeida, L., Masselink, G., Russell, P., Davidson, M., 2015. Observations of gravel beach dynamics during high energy wave conditions using a laser scanner. Geomorphology 228, 15–27. http://dx.doi.org/10.1016/j.geomorph.2014.08.019.

Anders, K., Lindenbergh, R.C., Vos, S.E., Mara, H., de Vries, S., Höfle, B., 2019. High-frequency 3D geomorphic observation using hourly terrestrial laser scanning data of a sandy beach. ISPRS Ann. Photogramm. Remote. Sens. Spat. Inf. Sci. IV-2-W5, 317–324.

Anders, K., Winiwarter, L., Höfle, B., 2021a. Improving change analysis from near-continuous 3D time series by considering full temporal information [Data and Source Code]. http://dx.doi.org/10.11588/data/1L11SQ.

Anders, K., Winiwarter, L., Höfle, B., 2022. Improving change analysis from near-continuous 3D time series by considering full temporal information. IEEE Geosci. Remote. Sens. Lett. 19, 1–5. http://dx.doi.org/10.1109/LGRS.2022.3148920.

Anders, K., Winiwarter, L., Lindenbergh, R.C., Williams, J.G., Vos, S.E., Höfle, B., 2020. 4D objects-by-change: Spatiotemporal segmentation of geomorphic surface change from LiDAR time series. ISPRS J. Photogramm. Remote Sens. 159, 352–363. http://dx.doi.org/10.1016/j.isprsjprs.2019.11.025.

Anders, K., Winiwarter, L., Mara, H., Lindenbergh, R.C., Vos, S.E., Höfle, B., 2021b. Fully automatic spatiotemporal segmentation of 3D LiDAR time series for the extraction of natural surface changes. ISPRS J. Photogramm. Remote Sens. 173, 297–308. http://dx.doi.org/10.1016/j.isprsjprs.2021.01.015.

Anegg, J., Fritzmann, P., 2019. Geomonitoring am felssturz im valsertal. URL: https://www.tirol.gv.at/fileadmin/themen/sicherheit/geoinformation/Monitoring/Vals_2019_Anegg_Fritzmann_Online.pdf.

Anon, 2014. Safety of Laser Products. Equipment Classification and Requirements. Technical Report, International Electro Technical Commission, URL: https://www.nen.nl/en/nen-en-iec-60825-1-2014-en-198247.

Arshad, B., Barthelemy, J., Perez, P., 2021. Autonomous lidar-based monitoring of coastal lagoon entrances. Remote. Sens. 13 (7), 1320.

Barbero-García, I., Kuschnerus, M., Vos, S., Lindenbergh, R., 2023. Automatic detection of bulldozer-induced changes on a sandy beach from video using YOLO algorithm. Int. J. Appl. Earth Obs. Geoinf. 117, 103185.

Berger, S., Hofmann, R., Wimmer, L., 2021. Einwirkungen auf starre barrieren durch fließähnliche gravitative massenbewegungen. Geotechnik 44 (2), 77–91. http://dx.doi.org/10.1002/gete.202000026.

Berndt, D.J., Clifford, J., 1994. Using dynamic time warping to find patterns in time series. In: Proceedings of the 3rd International Conference on Knowledge Discovery and Data Mining. Vol. 10, pp. 359–370.

Brocks, K., 1939. Vertikaler temperaturgradient und terrestrische refraktion, insbesondere im Hochgebirge. Veröffentlichungen Meteorol. Inst. Univ. Berl. 3 (4).

Brodie, K.L., Raubenheimer, B., Elgar, S., Slocum, R.K., McNinch, J.E., 2015. Lidar and pressure measurements of inner-surfzone waves and setup. J. Atmos. Ocean. Technol. 32 (10), 1945–1959.

Brodie, K.L., Slocum, R.K., McNinch, J.E., 2012. New insights into the physical drivers of wave runup from a continuously operating terrestrial laser scanner. In: 2012 Oceans. pp. 1–8. http://dx.doi.org/10.1109/OCEANS.2012.6404955.

Bucher, I., Wertheim, O., 2000. Measuring spatial vibration using continuous laser scanning. Shock. Vib. 7 (4), 203–208.

Campos, M., Junttila, S., Shcherbacheva, A., Wang, Y., Liang, X., Hyypä, J., Puttonen, E., 2021a. Perspectives on long-term TLS time-series to detect changes in tree crowns. In: Proceedings of the SilviLaser Conference 2021. pp. 105–107.

Campos, M., Litkey, P., Wang, Y., Chen, Y., Hyyti, H., Hyyppä, J., Puttonen, E., 2020. A terrestrial laser scanning measurement station to monitor long-term structural dynamics in a boreal forest. Int. Arch. Photogramm. Remote. Sens. Spat. Inf. Sci. XLIII-B1-2020, 27–31. http://dx.doi.org/10.5194/isprs-archives-XLIII-B1-2020-27-2020.

Campos, M.B., Litkey, P., Wang, Y., Chen, Y., Hyyti, H., Hyyppä, J., Puttonen, E., 2021b. A long-term terrestrial laser scanning measurement station to continuously monitor structural and phenological dynamics of boreal forest canopy. Front. Plant Sci. 11, http://dx.doi.org/10.3389/fpls.2020.606752.

Campos, M.B., Nunes, M.H., Shcherbacheva, A., Valve, V., Lintunen, A., Kaitaniemi, P., Junttila, S., Yann, S., Kulmala, M., Kukko, A., Hyyppä, J., Wang, Y., Puttonen, E., 2024. Factors and effects of inter-individual variability in silver birch phenology using dense LiDAR time-series. Agricult. Forest. Meterol. 358, 110253. http://dx.doi.org/10.1016/j.agrformet.2024.110253.

Campos, M., Valve, V., Shcherbacheva, A., Echriti, R., Wang, Y., Puttonen, E., 2023. Detection of silver birch growth dynamics and timing with dense spatio-temporal LiDAR time-series. Int. Arch. Photogramm. Remote. Sens. Spat. Inf. Sci. 48, 1715–1722.

Chebrolu, N., Läbe, T., Stachniss, C., 2020. Spatio-temporal non-rigid registration of 3D point clouds of plants. In: 2020 IEEE International Conference on Robotics and Automation. ICRA, pp. 3112–3118. http://dx.doi.org/10.1109/ICRA40945.2020.9197569.

Cheng, L., Chen, S., Liu, X., Xu, H., Wu, Y., Li, M., Chen, Y., 2018. Registration of laser scanning point clouds: A review. Sensors 18 (5), 1641.

Culvenor, D.S., Newnham, G.J., Mellor, A., Sims, N.C., Haywood, A., 2014. Automated in-situ laser scanner for monitoring Forest Leaf Area index. Sensors 14 (8), 14994–15008. http://dx.doi.org/10.3390/s140814994.

Czerwonka-Schröder, D., 2023. Konzeption einer qualitätsgesicherten Implementierung eines Echtzeitassistenzsystems basierend auf einem terrestrischen Long Range Laserscanner (Ph.D. thesis). Technische Universität Bergakademie Freiberg, Freiberg, Germany, Available at https://dgk.badw.de/fileadmin/user_upload/Files/DGK/docs/c-913.pdf.

Czerwonka-Schröder, D., Anders, K., Winiwarter, L., 2023a. Die permanente dreidimensionale datenerfassung alpiner hangrutschungen – multitemporale datenanalyse in webbasierten anwendungen. In: Weinold, T. (Ed.), 22. Internationale Geodätische Woche Obergurgl 2023. Wichmann, pp. 34–45.

Czerwonka-Schröder, D., Gaisecker, T., 2022. The permanent three-dimensional data acquisition of geotechnical structures by means of a web-based application of terrestrial LiDAR sensors. Geomech. Tunn. 15 (5), 596–604. http://dx.doi.org/10.1002/geot.202200012.

Czerwonka-Schröder, D., Kermarrec, G., Skytt, V., 2023b. Permanent LiDAR monitoring in alpine environments - web-based realtime guidance using analysis of multi-temporal datasets. In: Wieser, A. (Ed.), Ingenieurvermessung 23. Beiträge zum 20. Internationalen Ingenieurvermessungskurs Zürich. Wichmann, pp. 3–16.

Czerwonka-Schröder, D., Schulte, F., Albert, W., Hosseini, K., Tabernig, R., Yang, Y., Höfle, B., Holst, C., Zimmermann, K., 2025. Aimon5.0 - real-time monitoring of gravitational mass movements for critical infrastructure risk management with AI-assisted 3D metrology. In: Proceedings of the 6th Joint International Symposium on Deformation Monitoring (JISDM), Karlsruhe, Germany. http://dx.doi.org/10.5445/IR/1000179762.

Deruyter, G., De Sloover, L., Verbeurgt, J., De Wulf, A., 2020. Macrotidal beach monitoring (Belgium) using hypertemporal terrestrial lidar. In: Proc. FIG Working Week 2020, Amsterdam, the Netherlands. pp. 1–13.

Di Biase, V., Kuschnerus, M., Lindenbergh, R.C., 2022. Permanent laser scanner and synthetic aperture radar data: correlation characterisation at a sandy beach. Sensors 22 (6), 2311.

Eitel, J.U., Höfle, B., Vierling, L.A., Abellán, A., Asner, G.P., Deems, J.S., Glennie, C.L., Joerg, P.C., LeWinter, A.L., Magney, T.S., Mandlburger, G., Morton, D.C., Müller, J., Vierling, K.T., 2016. Beyond 3-D: The new spectrum of lidar applications for earth and ecological sciences. Remote Sens. Environ. 186, 372–392. http://dx.doi.org/10.1016/j.rse.2016.08.018.

Eitel, J.U., Vierling, L.A., Magney, T.S., 2013. A lightweight, low cost autonomously operating terrestrial laser scanner for quantifying and monitoring ecosystem structural dynamics. Agricult. Forest. Meterol. 180, 86–96. http://dx.doi.org/10.1016/j.agrformet.2013.05.012.

Eltner, A., Kaiser, A., Abellan, A., Schindewolf, M., 2017. Time lapse structure-from-motion photogrammetry for continuous geomorphic monitoring. Earth Surf. Process. Landf. 42 (14), 2240–2253. http://dx.doi.org/10.1002/esp.4178.

Förstner, W., Wrobel, B.P., 2016. Photogrammetric Computer Vision. Springer.

Fouché, G., Argelaguet, F., Faure, E., Kervrann, C., 2023. Immersive and interactive visualization of 3D spatio-temporal data using a space time hypercube: Application to cell division and morphogenesis analysis. Front. Bioinform. 3, 998991.

Friedli, E., 2020. Point Cloud Registration and Mitigation of Refraction Effects for Geomonitoring Using Long-Range Terrestrial Laser Scanning (Ph.D. thesis). ETH Zürich, Zurich, Switzerland, http://dx.doi.org/10.3929/ethz-b-000409052.

Gaisecker, T., Schröder, D., 2022. White Paper: RIEGL V-Line Scanners for Permanent Monitoring Applications and Integration Capabilities into Customers Risk Management. Technical Report, Riegl GmbH, Horn und Essen.

Goger, B., Stiperski, I., Nicholson, L., Sauter, T., 2022. Large-eddy simulations of the atmospheric boundary layer over an Alpine glacier: Impact of synoptic flow direction and governing processes. Q. J. R. Meteorol. Soc. http://dx.doi.org/10.1002/qj.4263.

Gojcic, Z., Litany, O., Wieser, A., Guibas, L.J., Birdal, T., 2021. Weakly supervised learning of rigid 3D scene flow. In: Proceedings of the IEEE/CVF Conference on Computer Vision and Pattern Recognition. pp. 5692–5703.

Handl, M., 2024. Solution for permanent monitoring based on RIEGL 3D terrestrial laser scanning. Geomech. Tunn. 17 (5), 395–401.

Hao, H., Wu, S., Li, Y., Wen, W., jiangchuan Fan, Zhang, Y., Zhuang, L., Xu, L., Li, H., Guo, X., Liu, S., 2024. Automatic acquisition, analysis and wilting measurement of cotton 3D phenotype based on point cloud. Biosyst. Eng. 239, 173–189. http://dx.doi.org/10.1016/j.biosystemseng.2024.02.010.

Hari, P., Kulmala, M., 2005. Station for measuring ecosystem-atmosphere relations (SMEAR II). Boreal Environ. Res. 10 (5), 315–322.

Hartl, S., 2019. Analyse der Felslawinen Frank Slide und Vals mit Hilfe des Computercodes r.avaflow (Master's thesis). Technische Universität Wien, http://dx.doi.org/10.34726/hss.2019.69060.

Hulskemper, D., Anders, K., Antolínez, J.A.Á., Kuschnerus, M., Höfle, B., Lindenbergh, R., 2022. Characterization OF morphological surface activities derived from near-continuous terrestrial LIDAR time series. Int. Arch. Photogramm. Remote. Sens. Spat. Inf. Sci. XLVIII-2/W2-2022, 53–60. http://dx.doi.org/10.5194/isprs-archives-XLVIII-2-W2-2022-53-2022.

Isenburg, M., 2013. LASzip: lossless compression of LiDAR data. Photogramm. Eng. Remote Sens. 79 (2), 209–217.

James, L.A., Hodgson, M.E., Ghoshal, S., Latiolais, M.M., 2012. Geomorphic change detection using historic maps and DEM differencing: The temporal dimension of geospatial analysis. Geomorphology 137 (1), 181–198.

Jin, J., Verbeurgt, J., De Sloover, L., Stal, C., Deruyter, G., Montreuil, A.-L., Vos, S., De Maeyer, P., De Wulf, A., 2021a. Monitoring spatiotemporal variation in beach surface moisture using a long-range terrestrial laser scanner. ISPRS J. Photogramm. Remote Sens. 173, 195–208.

Jin, J., Verbeurgt, J., De Sloover, L., Stal, C., Deruyter, G., Montreuil, A.-L., Vos, S., De Maeyer, P., De Wulf, A., 2021b. Support vector regression for high-resolution beach surface moisture estimation from terrestrial LiDAR intensity data. Int. J. Appl. Earth Obs. Geoinf. 102, 102458.

Junttila, S., Campos, M., Hölttä, T., Lindfors, L., El Issaoui, A., Vastaranta, M., Hyyppä, H., Puttonen, E., 2022. Tree water status affects tree branch position. Forests 13 (5), http://dx.doi.org/10.3390/f13050728.

Kellerer-Pirklbauer, A., Bauer, A., Proske, H., 2005. Terrestrial laser scanning for glacier monitoring: Glaciation changes of the Gößnitzkees glacier (Schober group, Austria) between 2000 and 2004. In: Proceedings of the 3rd Symposium of the Hohe Tauern National Park for Research in Protected Areas, Kaprun, Austria. pp. 97–106.

Kermarrec, G., Yang, Z., Czerwonka-Schröder, D., 2022. Classification of terrestrial laser scanner point clouds: A comparison of methods for landslide monitoring from mathematical surface approximation. Remote. Sens. 14 (20), 5099.

Kohonen, T., 1990. The self-organizing map. Proc. IEEE 78 (9), 1464–1480. http://dx.doi.org/10.1109/5.58325.

Kreutz, T., Mühlhäuser, M., Guinea, A.S., 2023. Unsupervised 4D LiDAR moving object segmentation in stationary settings with multivariate occupancy time series. In: Proceedings of the IEEE/CVF Winter Conference on Applications of Computer Vision. pp. 1644–1653.

Kromer, R.A., Abellán, A., Hutchinson, D.J., Lato, M., Chanut, M.-A., Dubois, L., Jaboyedoff, M., 2017. Automated terrestrial laser scanning with near-real-time change detection – monitoring of the séchilienne landslide. Earth Surf. Dyn. 5 (2), 293–310. http://dx.doi.org/10.5194/esurf-5-293-2017.

Kromer, R.A., Abellán, A., Hutchinson, D.J., Lato, M., Edwards, T., Jaboyedoff, M., 2015. A 4D filtering and calibration technique for small-scale point cloud change detection with a terrestrial laser scanner. Remote. Sens. 7 (10), 13029–13052. http://dx.doi.org/10.3390/rs71013029.

Kuschnerus, M., de Vries, S., Antolínez, J.A., Vos, S., Lindenbergh, R., 2024b. Identifying topographic changes at the beach using multiple years of permanent laser scanning. Coast. Eng. 104594.

Kuschnerus, M., Lindenbergh, R., Vos, S., 2021a. Coastal change patterns from time series clustering of permanent laser scan data. Earth Surf. Dyn. 9 (1), 89–103.

Kuschnerus, M., Lindenbergh, R., Vos, S., Hanssen, R., 2024a. Statistically assessing vertical change on a sandy beach from permanent laser scanning time series. ISPRS Open J. Photogramm. Remote. Sens. 11, 100055. http://dx.doi.org/10.1016/j.ophoto.2023.100055.

Kuschnerus, M., Schröder, D., Lindenbergh, R., 2021b. Environmental influences on the stability of a permanently installed laser scanner. In: The International Archives of the Photogrammetry, Remote Sensing and Spatial Information Sciences. Vol. XLIII-B2-2021, Copernicus GmbH, pp. 745–752. http://dx.doi.org/10.5194/isprs-archives-XLIII-B2-2021-745-2021.

Lague, D., Brodu, N., Leroux, J., 2013. Accurate 3D comparison of complex topography with terrestrial laser scanner: Application to the Rangitikei canyon (N-Z). ISPRS J. Photogramm. Remote Sens. 82, 10–26. http://dx.doi.org/10.1016/j.isprsjprs.2013.04.009.

Lindenbergh, R., van der Kleij, S., Kuschnerus, M., Vos, S., de Vries, S., 2019. Clustering time series of repeated scan data of sandy beaches. Int. Arch. Photogramm. Remote. Sens. Spat. Inf. Sci. XLII-2/W13, 1039–1046. http://dx.doi.org/10.5194/isprs-archives-XLII-2-W13-1039-2019.

Malsam, A., Walton, G., Schovanec, H., Bonneau, D., DiFrancesco, P., Hutchinson, D., 2021. An analysis of seasonal rockfall trends at floyd hill: A slope along I-70, East of Idaho Springs, CO. In: ARMA US Rock Mechanics/Geomechanics Symposium. ARMA, pp. 1–12.

Marchand, L.J., Dox, I., Gričar, J., Prislan, P., Leys, S., Van den Bulcke, J., Fonti, P., Lange, H., Matthysen, E., Peñuelas, J., Zuccarini, P., Campioli, M., 2020. Inter-individual variability in spring phenology of temperate deciduous trees depends on species, tree size and previous year autumn phenology. Agricult. Forest. Meterol. 290, 108031. http://dx.doi.org/10.1016/j.agrformet.2020.108031.

Monji-Azad, S., Hesser, J., Löw, N., 2023. A review of non-rigid transformations and learning-based 3D point cloud registration methods. ISPRS J. Photogramm. Remote Sens. 196, 58–72.

Monserrat, O., Crosetto, M., Luzi, G., 2014. A review of ground-based SAR interferometry for deformation measurement. ISPRS J. Photogramm. Remote Sens. 93, 40–48.

Montillet, J.-P., Kermarrec, G., Forootan, E., Haberreiter, M., He, X., Finsterle, W., Fernandes, R., Shum, C.K., 2024. How big data can help to monitor the environment and to mitigate risks due to climate change: A review. IEEE Geosci. Remote. Sens. Mag. 12 (2), 67–89. http://dx.doi.org/10.1109/MGRS.2024.3379108.

Myronenko, A., Song, X., 2010. Point set registration: Coherent point drift. IEEE Trans. Pattern Anal. Mach. Intell. 32 (12), 2262–2275. http://dx.doi.org/10.1109/TPAMI.2010.46.

O'Dea, A., Brodie, K.L., Hartzell, P., 2019. Continuous Coastal monitoring with an automated terrestrial lidar scanner. J. Mar. Sci. Eng. 7 (2), http://dx.doi.org/10.3390/jmse7020037.

Pesci, A., Teza, G., 2008. Terrestrial laser scanner and retro-reflective targets: an experiment for anomalous effects investigation. Int. J. Remote Sens. 29 (19), 5749–5765. http://dx.doi.org/10.1080/01431160802108489.

Pirotti, F., 2019. Open software and standards in the realm of laser scanning technology. Open Geospatial Data Softw. Stand. 4, 1–13. http://dx.doi.org/10.1186/s40965-019-0073-z.

Puttonen, E., Lehtomäki, M., Litkey, P., Näsi, R., Feng, Z., Liang, X., Wittke, S., Pandžic, M., Hakala, T., Karjalainen, M., Pfeifer, N., 2019. A clustering framework for monitoring circadian rhythm in structural dynamics in plants from terrestrial laser scanning time series. Front. Plant Sci. 10, http://dx.doi.org/10.3389/fpls.2019.00486.

Py4dgeo Development Core Team, 2022. Py4dgeo: library for change analysis in 4D point clouds. URL: https://github.com/3dgeo-heidelberg/py4dgeo. MIT License, version 0.5.0.

RIEGL, 2019a. Datasheet RIEGL VZ-6000. RIEGL Laser Measurement Systems, Horn, Austria.

RIEGL, 2019b. RiSCAN PRO, 2.8.0 ed. RIEGL Laser Measurement Systems, Horn, Austria.

RIEGL, 2024. ROS2 RIEGL VZ package. URL: https://github.com/rieglms/ros-riegl-vz.

Ruttner, P., Glaus, J., Wieser, A., Bühler, Y., 2023. A measurement system for mapping snow distribution changes in an avalanche release zone. In: International Snow Science Workshop. ISSW 2023, Montana State University Library, pp. 1074–1081.

Ruttner, P., Voordendag, A., Hartmann, T., Glaus, J., Wieser, A., Bühler, Y., 2024. Monitoring snow depth variations in an avalanche release area using low cost LiDAR and optical sensors. EGUsphere 2024, 1–20. http://dx.doi.org/10.5194/egusphere-2024-744, URL: https://egusphere.copernicus.org/preprints/2024/egusphere-2024-744/.

Schröder, D., Anders, K., Winiwarter, L., Wujanz, D., 2022. Permanent terrestrial LiDAR monitoring in mining, natural hazard prevention and infrastructure protection—Chances, risks, and challenges: A case study of a rockfall in Tyrol, Austria. In: Proceedings of the 5th Joint International Symposium on Deformation Monitoring (JISDM), Valencia, Spain. pp. 20–22.

Schunck, D., Magistri, F., Rosu, R.A., Cornelißen, A., Chebrolu, N., Paulus, S., Léon, J., Behnke, S., Stachniss, C., Kuhlmann, H., et al., 2021. Pheno4D: A spatio-temporal dataset of maize and tomato plant point clouds for phenotyping and advanced plant analysis. PLOS ONE 16 (8), e0256340.

Shcherbacheva, A., Campos, M.B., Wang, Y., Liang, X., Kukko, A., Hyyppä, J., Junttila, S., Lintunen, A., Korpela, I., Puttonen, E., 2024. A study of annual tree-wise LiDAR intensity patterns of boreal species observed using a hyper-temporal laser scanning time series. Remote Sens. Environ. 305, 114083. http://dx.doi.org/10.1016/j.rse.2024.114083.

Soudarissanane, S., Lindenbergh, R., Menenti, M., Teunissen, P., 2011. Scanning geometry: Influencing factor on the quality of terrestrial laser scanning points. ISPRS J. Photogramm. Remote Sens. 66 (4), 389–399. http://dx.doi.org/10.1016/j.isprsjprs.2011.01.005.

Spadavecchia, C., Campos, M.B., Piras, M., Puttonen, E., Shcherbacheva, A., 2023. Wood-leaf unsupervised classification of silver birch trees for biomass assessment using oblique point clouds. Int. Arch. Photogramm. Remote. Sens. Spat. Inf. Sci. 48, 1795–1802.

Suchde, P., Kuhnert, J., 2018. Point cloud movement for fully Lagrangian meshfree methods. J. Comput. Appl. Math. 340, 89–100.

Van IJzendoorn, C., Boomaars, K., Vos, S., Reniers, A., Kuschnerus, M., Lindenbergh, R., 2024. Detection and characterization of aeolian sand strips on the beach using permanent laser scanning. Geomorphica 1 (1), http://dx.doi.org/10.59236/geomorphica.v1i1.32.

Vo, A.-V., Truong-Hong, L., Laefer, D.F., Bertolotto, M., 2015. Octree-based region growing for point cloud segmentation. ISPRS J. Photogramm. Remote Sens. 104, 88–100.

Voordendag, A.B., Goger, B., Klug, C., Prinz, R., Rutzinger, M., Kaser, G., 2021. Automated and permanent long-range terrestrial laser scanning in a high mountain environment: Setup and first results. ISPRS Ann. Photogramm. Remote. Sens. Spat. Inf. Sci. V-2-2021, 153–160. http://dx.doi.org/10.5194/isprs-annals-V-2-2021-153-2021.

Voordendag, A.B., Goger, B., Klug, C., Prinz, R., Rutzinger, M., Kaser, G., 2022. The stability of a permanent terrestrial laser scanning system – a case study with hourly scans. Int. Arch. Photogramm. Remote. Sens. Spat. Inf. Sci. XLIII-B2-2022, 1093–1099. http://dx.doi.org/10.5194/isprs-archives-XLIII-B2-2022-1093-2022.

Voordendag, A., Goger, B., Klug, C., Prinz, R., Rutzinger, M., Sauter, T., Kaser, G., 2023a. Uncertainty assessment of a permanent long-range terrestrial laser scanning system for the quantification of snow dynamics on Hintereisferner (Austria). Front. Earth Sci. 11, http://dx.doi.org/10.3389/feart.2023.1085416.

Voordendag, A., Goger, B., Prinz, R., Sauter, T., Mölg, T., Saigger, M., Kaser, G., 2024. A novel framework to investigate wind-driven snow redistribution over an alpine glacier: combination of high-resolution terrestrial laser scans and large-eddy simulations. Cryosphere 18 (2), 849–868. http://dx.doi.org/10.5194/tc-18-849-2024.

Voordendag, A., Prinz, R., Schuster, L., Kaser, G., 2023b. Brief communication: The Glacier Loss Day as an indicator of a record-breaking negative glacier mass balance in 2022. Cryosphere 17 (8), 3661–3665. http://dx.doi.org/10.5194/tc-17-3661-2023.

Vos, S., Anders, K., Kuschnerus, M., Lindenbergh, R., Höfle, B., Aarninkhof, S., de Vries, S., 2021. A six month high resolution 4D geospatial stationiary laser scan dataset of the Kijkduin beach dune system, The Netherlands. http://dx.doi.org/10.1594/PANGAEA.934058.

Vos, S., Anders, K., Kuschnerus, M., Lindenbergh, R., Höfle, B., Aarninkhof, S., de Vries, S., 2022. A high-resolution 4D terrestrial laser scan dataset of the Kijkduin beach-dune system, The Netherlands. Sci. Data 9 (1), 1–11.

Vos, S., De Sloover, L., Lindenbergh, R., De Wulf, A., 2024. A high-resolution 4D geospatial laser scan dataset of the beach at Mariakerke Bad, Belgium. http://dx.doi.org/10.5281/zenodo.10433522.

Vos, S., Kuschnerus, M., Lindenbergh, R., de Vries, S., 2023. 4D spatio-temporal laser scan dataset of the beach-dune system in Noordwijk, NL. http://dx.doi.org/10.4121/1AAC46FB-7900-4D4C-A099-D2CE354811D2.V2.

Vosselman, G., Maas, H. (Eds.), 2010. Airborne and Terrestrial Laser Scanning. CRC Press, United Kingdom.

Vousdoukas, M., Kirupakaramoorthy, T., Oumeraci, H., de la Torre, M., Wübbold, F., Wagner, B., Schimmels, S., 2014. The role of combined laser scanning and video techniques in monitoring wave-by-wave swash zone processes. Coast. Eng. 83, 150–165. http://dx.doi.org/10.1016/j.coastaleng.2013.10.013.

Wang, D., Puttonen, E., Casella, E., 2022. PlantMove: A tool for quantifying motion fields of plant movements from point cloud time series. Int. J. Appl. Earth Obs. Geoinf. 110, 102781. http://dx.doi.org/10.1016/j.jag.2022.102781.

Weidner, L., van Veen, M., Lato, M., Walton, G., 2021. An algorithm for measuring landslide deformation in terrestrial lidar point clouds using trees. Landslides 18, 3547–3558.

Williams, J.G., Rosser, N.J., Hardy, R.J., Brain, M.J., Afana, A.A., 2018. Optimising 4-D surface change detection: an approach for capturing rockfall magnitude–frequency. Earth Surf. Dyn. 6 (1), 101–119. http://dx.doi.org/10.5194/esurf-6-101-2018.

Winiwarter, L., Anders, K., Czerwonka-Schröder, D., Höfle, B., 2023. Full four-dimensional change analysis of topographic point cloud time series using Kalman filtering. Earth Surf. Dyn. 11 (4), 593–613.

Winiwarter, L., Anders, K., Höfle, B., 2021. M3C2-EP: Pushing the limits of 3D topographic point cloud change detection by error propagation. ISPRS J. Photogramm. Remote Sens. 178, 240–258.

Winiwarter, L., Esmorís Pena, A.M., Weiser, H., Anders, K., Martínez Sánchez, J., Searle, M., Höfle, B., 2022. Virtual laser scanning with HELIOS++: a novel take on ray tracing-based simulation of topographic 3D laser scanning. Remote Sens. Environ. 269, 112772. http://dx.doi.org/10.1016/j.rse.2021.112772.

Wittke, S., Campos, M., Ruoppa, L., Echriti, R., Wang, Y., Gołoś, A., Kukko, A., Hyyppä, J., Puttonen, E., 2024. LiPheStream-A 18-month high spatiotemporal resolution point cloud time series of boreal trees from Finland. Sci. Data 11 (1), 1281.

Yang, Y., Czerwonka-Schröder", D., Seufert, P., Holst, C., 2025. Using point cloud registration to mitigate systematic errors in permanent laser scanning-based landslide monitoring. In: Proceedings of the 6th Joint International Symposium on Deformation Monitoring. JISDM, pp. 1–9.

Yang, Y., Schwieger, V., 2022. Supervoxel-based targetless registration and identification of stable areas for deformed point clouds. J. Appl. Geod. http://dx.doi.org/10.1515/jag-2022-0031.

Yrttimaa, T., Junttila, S., Luoma, V., Pyörälä, J., Puttonen, E., Campos, M., Hölttä, T., Vastaranta, M., 2024. Tree height and stem growth dynamics in a scots pine dominated boreal forest. Trees For. People 15, 100468.

Zahs, V., Winiwarter, L., Anders, K., Williams, J.G., Rutzinger, M., Höfle, B., 2022. Correspondence-driven plane-based M3C2 for lower uncertainty in 3D topographic change quantification. ISPRS J. Photogramm. Remote Sens. 183, 541–559.

Zhang, X., Zhang, M., Jiang, L., Yue, P., 2020. An interactive 4D spatio-temporal visualization system for hydrometeorological data in natural disasters. Int. J. Digit. Earth 13 (11), 1258–1278.

Zoumpekas, T., Puig, A., Salamó, M., García-Sellés, D., Blanco Nuñez, L., Guinau, M., 2021. An intelligent framework for end-to-end rockfall detection. Int. J. Intell. Syst. 36 (11), 6471–6502. http://dx.doi.org/10.1002/int.22557.